2017

SYNTHESIS AND DEVELOPMENT OF ZWITTERIONIC PEI (zPEI) FOR OPTIMIZED DELIVERY OF NUCLEIC ACIDS

Joseph Raleigh Duke III
University of Kentucky, joseph.duke@uky.edu
Digital Object Identifier: https://doi.org/10.13023/ETD.2017.452

STUDENT AGREEMENT:

I represent that my thesis or dissertation and abstract are my original work. Proper attribution has been given to all outside sources. I understand that I am solely responsible for obtaining any needed copyright permissions. I have obtained needed written permission statement(s) from the owner(s) of each third-party copyrighted matter to be included in my work, allowing electronic distribution (if such use is not permitted by the fair use doctrine) which will be submitted to UKnowledge as Additional File.

I hereby grant to The University of Kentucky and its agents the irrevocable, non-exclusive, and royalty-free license to archive and make accessible my work in whole or in part in all forms of media, now or hereafter known. I agree that the document mentioned above may be made available immediately for worldwide access unless an embargo applies.

I retain all other ownership rights to the copyright of my work. I also retain the right to use in future works (such as articles or books) all or part of my work. I understand that I am free to register the copyright to my work.

REVIEW, APPROVAL AND ACCEPTANCE

The document mentioned above has been reviewed and accepted by the student's advisor, on behalf of the advisory committee, and by the Director of Graduate Studies (DGS), on behalf of the program; we verify that this is the final, approved version of the student's thesis including all changes required by the advisory committee. The undersigned agree to abide by the statements above.

Joseph Raleigh Duke III, Student

Dr. Jason DeRouchey, Major Professor

Dr. Mark Lovell, Director of Graduate Studies

SYNTHESIS AND DEVELOPMENT OF ZWITTERIONIC PEI (zPEI) FOR OPTIMIZED DELIVERY OF NUCLEIC ACIDS

THESIS

A thesis submitted in partial fulfillment of the
requirements for the degree of Master of Science in the
College of Arts and Sciences
at the University of Kentucky

By

Joseph Raleigh Duke III

Lexington, Ky

Director: Dr. Jason DeRouchey, Professor of Chemistry

Lexington, Ky

2017

ABSTRACT OF THESIS

SYNTHESIS AND DEVELOPMENT OF ZWITTERIONIC PEI (zPEI) FOR OPTIMIZED DELIVERY OF NUCLEIC ACIDS

Gene therapy holds promise for the treatment a wide range of diseases ranging from cystic fibrosis to cardiovascular disease to cancer. The need for safe and efficient gene delivery methods remains the primary barrier to human gene therapy. Non-viral vector materials, including polymers, can be designed to be biocompatible and non-immunogenic, but lack the efficiency to be clinically relevant. Gene therapy awaits the development of new materials that are both safe and efficient. Here, we have synthesized a series of modified zwitterionic polymers based on the common transfecting agent polyethylenimine (PEI). Using a variety of biochemical and biophysical methods we have studied structure-function relation in zPEI-DNA as a function of percent modification. Our results show significant structural rearrangements in the DNA condensates with increasing zwitterionic character. The percent zwitterionic modification determines not only DNA packaging but the serum stability of the resulting polyplexes with more highly modified zPEI releasing DNA more readily.

KEYWORDS: Chemical Transfection Agents, Gene Therapy, Zwitterionic Modifications, Biophysical Characterization, DNA Condensation

Joseph Raleigh Duke III

November 6, 2017

SYNTHESIS AND DEVELOPMENT OF ZWITTERIONIC PEI (zPEI) FOR OPTIMIZED DELIVERY OF NUCLEIC ACIDS

By

Joseph Raleigh Duke III

Dr. Jason DeRouchey

Director of Thesis

Dr. Mark Lovell

Director of Graduate Studies

November 21, 2017

ACKNOWLEDGEMENTS

I would like to thank my advisor Dr. Jason DeRouchey for his mentorship, guidance, and understanding throughout my graduate studies. Additionally, I would like to acknowledge my group members Daniel Kirchoff, Xiaolu Zhang, Min An, Cody Gay, Kanthi Nuti, Ehigbai Oikeh, Iris Begum, Kyle Starkey, Emily Fryman, and Leslie Uche for their support, assistance, and friendship. Dr. Sean Parkin was instrumental in setting up the small angle x-ray scattering experiments, and I am thankful for his time and expertise. I am very appreciative of the assistance and perspective I was given by members of the labs of Dr. Richards, Dr. Glazer, Dr. Miller, and Dr. Kim. Furthermore, I am grateful to the University of Kentucky Chemistry Department and all the wonderful people I met during my time here. I would like to thank Logan Warriner and Dr. Daniel Pack (UK Chemical and Materials Engineering) for their collaboration on the modified PEI project, and Johann Hansing and Dr. Roland Netz (Free University of Berlin) for their work on the mixed charged diffusion project.

Finally, I would like to thank my friends and family for their love and support over the course of my graduate studies and for sticking with me through the experience.

TABLE OF CONTENTS

LIST OF TABLES

LIST OF FIGURES

Chapter 1: Introduction

1.1. Introduction to Gene Delivery by Chemical Transfectors

Many human diseases result from mutations in genetic material that lead to poor regulation of gene expression or transcription and translation of flawed proteins. For example, cancer is caused by mutations in oncogenes, which leads to unregulated cellular proliferation[1]. Cystic fibrosis results from an inherited mutation to the gene encoding CFTR, a chlorine ion channel, which leads to mucus buildup affecting lung function[2]. Other than treatment of symptoms, increasing understandings of the genetic origins of disease has promoted efforts to modulate expression or introduce non-pathogenic copies of genes[3]. Additionally, introduction of genetic materials into cell cultures and animal models has become invaluable to the study of protein function as well as study of disease and therapeutics[4]. While the gene therapy field once showed great potential, the small number of clinical trials and lack of pharmaceutical application has resulted from inadequacies in current delivery techniques.[5-6] In order to be effective in treatment, a gene carrier must be nontoxic, must protect the gene from extracellular and intracellular degradation, must be able to deliver the gene into the cells of interest, and must release its cargo into the nucleus or cytoplasm so that it can be transcribed.[5, 7]

Existing transfection techniques can be grouped into two categories: viral and non-viral. Because viruses have been subject to natural selection, they have evolved with characteristics to overcome the major obstacles of transporting DNA into a host cell.[5] While viral based vectors sport very high transfection efficiencies, their widespread use is limited due to a variety of factors. Both adenovirus and retrovirus derived vectors suffer from risk of contamination with an active "helper" virus, and limitations in size of DNA

payload.[8-9] Adenoviral vectors currently are limited in efficiency, partially due to being limited by the cell host's life cycle.[8] Retrovirus derived vectors suffer from risk of immunogenic response, of accidental infection with a self-replicating virus, and of faulty replication of the gene of interest by reverse transcriptase.[9] Such an error could result in higher expression of a faulty gene, worsening or accelerating the targeted disease. These concerns have been amplified by the death of early participants in clinical trials, such as Jesse Gelsinger, who died in 1999 as a result of viral injection in an attempt to cure his ornithine transcarbamylase deficiency (OTC), setting viral delivery research back as a result of the public backlash. [10] Physical methods such as microinjections or electroporation show limitations in efficacy due to potential for cellular damage.[7] In addition, they are often low throughput, and difficult to apply to organisms of high cellular diversity.[7] While current chemical agents show lower efficiencies than viral vectors, their reduced risk of immunogenicity along with large variability in chemical structure and ease of production give them high potential as gene carriers.[5, 7]

Cationic polymers, such as polyethylenimine (PEI) and polyamidoamide (PAMAM), along with peptides and lipid carriers, are among the most well studied chemical transfection agents.[7] A commonality between the major chemical transfectors is the ability to interact with and bind to DNA through electrostatic interaction with the negative phosphate backbone.[4-5, 11] While lipid carriers, such as lipofectamine, are well established transfection agents for laboratory cell work, poor performance in vivo, as well as difficulty of consistent sample preparations limit their application in a clinical setting.[5, 11] Cationic polymers, such as polyethylenimine (PEI) and polyamidoamine (PAMAM), suffer from high cellular toxicity and low transfection efficiency when compared with viral

vectors, but their use carries a much lower risk of infection or of an immune response.[5] Because their chemical structures and properties are readily tunable, a great potential exists for optimization of commercially available cationic polymers for transfection.[5] While it is clear that a relationship exists between the structure of chemical agents and their ability to deliver DNA for expression, the field still lacks rigorous characterization of the parameters that lead to transfection. Previous research has shown improved transfection efficiency and cytotoxicity in polyplexes, polycation-DNA complexes, by reducing nonspecific interactions with proteins, blood and other biological components; in addition to loosening the strength of the interaction between the polymer and the nucleic acid payload, to facilitate more efficient cellular release.[12-25] This has been accomplished through addition of charge neutral hydrophilic groups such as PEG by grafting, use of negatively charged copolymers, reduction of charge by covalent modification, and through addition of hydrolysable charge shifting groups.[12-25] A better understanding of how such alterations modulate the properties of interaction between chemical agents and their nucleic acid payload is needed for continued progress in creating improved molecules for gene delivery.

Previous work by the DeRouchey group has shown, surprisingly, that mixed charge peptides are capable of condensing DNA. The resulting DNA packaging is influenced by both the number and chemical nature of the negative moiety. In this thesis, we have modified a commercial 25 kDa branched polyethyleneimine (bPEI) polymer through reaction with succinic anhydride to form mixed charge, or zwitterionic, PEI (zPEI). By modulating the ratio of PEI to succinic anhydride, a series of zPEI were synthesized with varying degrees of modification through reaction of succinic anhydride with primary and secondary amines on bPEI. With a combination of structural studies in addition to cell

work performed by collaborators in the laboratory of Dr. Dan Pack (University of Kentucky, Chemical and Materials Engineering), we have explored how the percent modification of zPEI affects the binding, protection, and release properties, as well as the packaging density of the resulting polyplexes. Our hypothesis is that zwitterionic PEI will provide the ability to systematically tune polymer-DNA interactions leading to polyplexes with enhanced intracellular unpackaging and more efficient gene delivery. At high percent modification, we anticipate the polymer-DNA interactions are too weak for effective DNA delivery, thus an optimal ratio of modification should be determined for zPEI. Generally, for nonviral delivery of polymers, a large excess of polycation (typically amine based) must be used to form stable colloidal nanoparticles suitable for DNA delivery. As these polycations are generally toxic to cells, we also hypothesize zPEI will result in polymer carriers with reduced cellular toxicity. This chapter will broadly review existing literature on polycationic transfection agents. The following chapters will detail the synthesis and characterization of the zwitterionic PEI (zPEI) along with biophysical characterization (chapter 2) and x-ray studies on DNA polyplex formation (chapter 3).

1.2. Structure of Polymer Based Transfection Agents

The structures of several common variants of chemical transfectors are shown in figure 1.1. This work focuses on the cationic polymer transfectors, which will be discussed in greater detail. Polylysine, one of the first cationic polymers proposed to be used for delivery of genetic material, is simply a chain of the amino acid lysine conjoined by peptide bonds between the α-amino and α-carboxylic group of adjacent lysine residues.[26] The net positive charge of the polymer results from the lysyl group containing a primary amine.

Polyethylenimine (PEI), one of the most well established chemical transfection agents, is made up of repeating ethylendiamine units. PEI exhibits high transfection efficiency compared to many other polymers and is often considered as a "gold standard" in gene delivery. Commercially available PEI is often characterized in two ways; by the average molecular weight of individual polymer chains, and by the presence or absence of branching in the molecule.[27] As pictured in figure 1.1, PEI can be either linear (lPEI) or branched (bPEI). The amine groups lend a high positive charge to the molecules at physiological pH. The branched form of PEI (bPEI) contains a combination of primary, secondary, and tertiary amines, and the linear form predominantly contains secondary amines. PEI used throughout this work, 25 kDa bPEI, has been shown by C^{13} NMR analysis to contain roughly 31% primary, 39% secondary, and 30% tertiary amines.[28] bPEI is thought to be especially effective due to the presence of these secondary and tertiary amines, which provide buffering capability over a wide range of pH.[29] Acid titration studies of branched PEI reveal broad pKa distributions.[29] Because PEIs are made up of neighboring amine groups, both the covalent linkage and the close proximity of adjacent

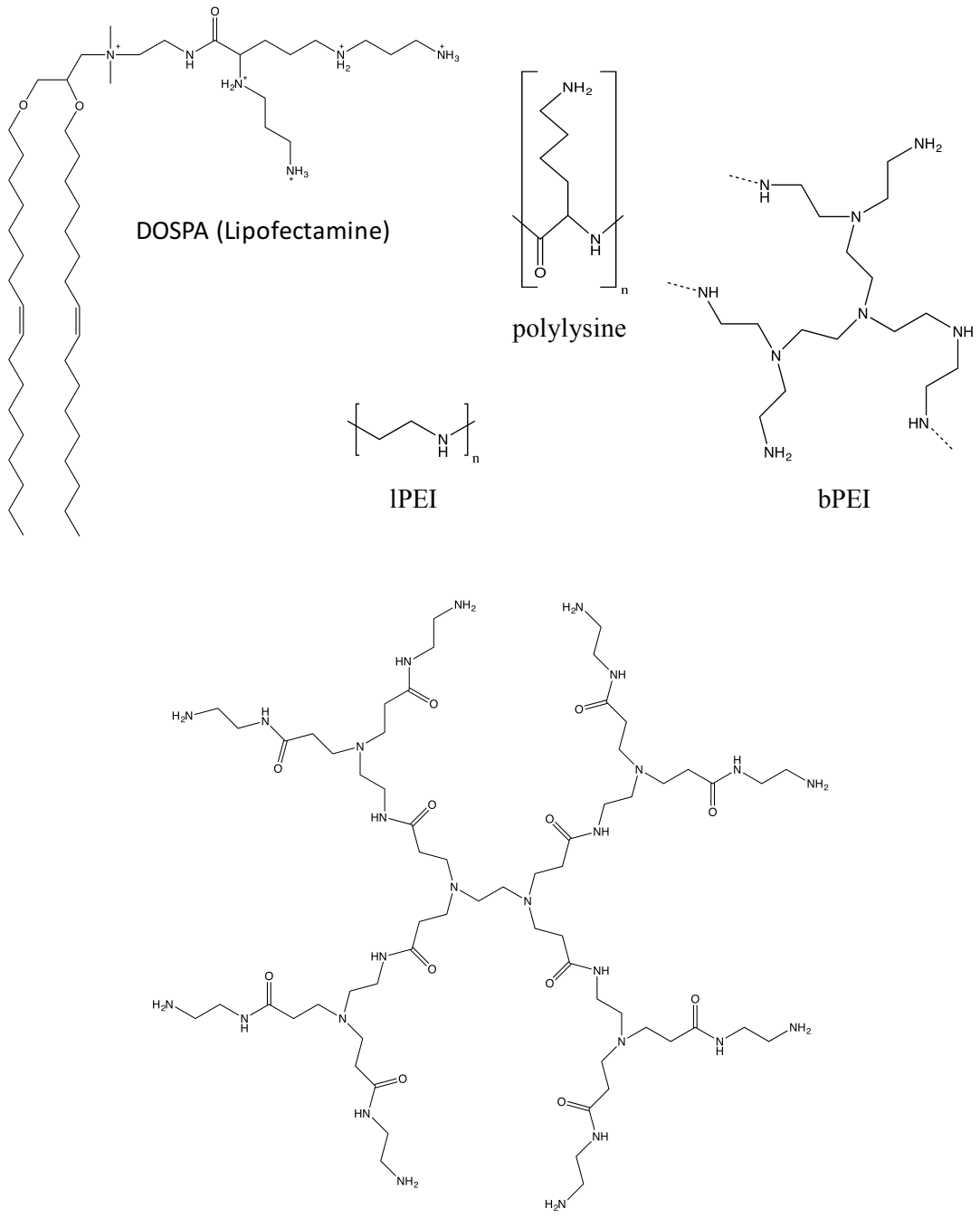

Figure 1.1. Structures of common polymer transfection agents.

branches alters the pKa of neighboring amines.[22, 29] A simplistic example can be seen for a single ethylenediamine, a symmetric molecule made up of an ethyl group with single primary amines attached to each carbon. However, these two, seemingly identical, nitrogen have different pKas (9.98 and 7.52).[29] As the first amine protonates below pH 9.98, the pKa of the unprotonated nitrogen decreases due to the proximity to the charged amine. Because of the random branching structure and large number of amines per molecule of PEI, the individual pKas and orders of protonation/deprotonation are not well established, but mathematical fits of titration data on 500 kDa branched PEI estimate that at a physiological pH, roughly 80-90% of nitrogen are uncharged.[29] Another group, who studied a 10 kDa variant of bPEI, reported that 70% of nitrogens remained uncharged at pH 7.4.[30] The wide range of pKas of PEI nitrogen make the molecules good physiological buffers.

Polyamidoamine (PAMAM), another commercially available cationic transfection agent, differs from both branched and linear PEI in that it is a dendrimer.[5, 31] Dendrimers are named for their branched, "tree like" structure, and are made up of repeating, radial symmetric branched units around a central "core" molecule.[31-32] Because of their high degree of symmetry, and tight control over parameters, such as surface chemistry and number of surface groups, dendrimers represent a potential alternative to linear and disordered branch structures for use in DNA polyplex assembly and delivery. Higher generation PAMAM dendrimers are thought to be spherical in form and terminate with an outer layer of primary amine groups.[31] PAMAM dendrimers are typically synthesized by

a divert method through a repeating two-step reaction process, a Michael addition followed by amidation, that results in two new branches off of every primary surface amine. [31-32] Every cycle of these reactions is referred to as a new generation, where the number of reactive surface groups is double the previous generation.[31] For example, if the reaction is terminated after the first cycle on an ethylenediamine (bifunctional) core, the resulting polymer will be termed PAMAM G0, for generation 0 and have 4 primary amines on its surface. If the Michael addition/amidation cycle is repeated 4 times, the product will be third generation PAMAM (G3 PAMAM) and have 32 primary amine surface groups. PAMAM G1 is presented in figure 1.1. G4 PAMAM was used in this study with 64 surface amine groups. Titration experiments have shown that the outer primary amines of G4 have pKas of 9.9, thus possessing charge at physiological pH.[33] The effective charge of G4 PAMAM however is expected to be less than +64. Tertiary amines have pKas of ~6.5, and non-surface group amines of PAMAM are thus believed to be uncharged at physiological pH. At low pH, such as that found in lysosomes, these tertiary amines may be charged. [33-34] Like PEI, PAMAM dendrimers are good physiological buffers.[34]

1.3. Mechanism of DNA Binding and Delivery

Efficient delivery of nucleic acids for non-viral gene therapies must include means to successfully navigate several kinetic and energetic barriers; including effective compaction and particle stability of the polyplexes to be efficiently internalized by cells

yet sufficiently labile to subsequently release the nucleic acids for delivery.[5] A simple cartoon depicting the barriers to cell transfection is displayed below in figure 1.2.

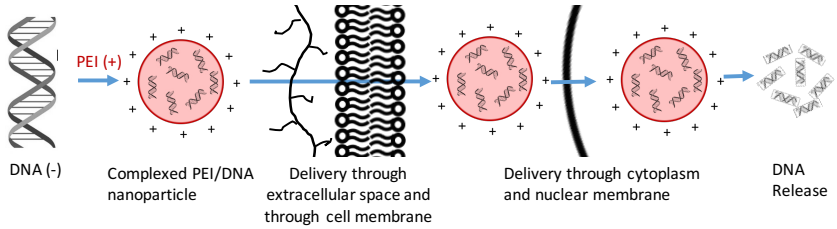

Figure 1.2. Cellular barriers for effective chemical transfection

The first barrier a chemical transfector must navigate is transportation and protection of the nucleic acids through a tightly regulated and degradative extracellular environment. Naked nucleic acids are not capable of effectively crossing the cell membrane due to their large size and charge. To overcome this barrier, various condensing agents have been successfully used to create nanometer sized complexes capable of more readily carrying nucleic acids across the cell membrane.[35] Additionally, degradative enzymes, such as DNAse, which are present extracellularly and intracellularly, severely limit the time that cell targets are exposed to unprotected genes.[36-37] Condensing agents, such as PEI, also prevent DNA degradation in cells for several hours.[5, 36] DNA particles bind to polycations spontaneously in dilute aqueous solutions forming nanometer scale particles called polyplexes.[4-5, 11, 38-39] Interactions between DNA and polymer are the result of electrostatic forces between the negative DNA backbone and the positively charged groups on the polymer.[7] It is believed that this process is made entropically favorable by the release of counter-ions from the oppositely charged molecules into solution.[40-41] Polyplexes are often found to have the highest transfection efficiencies when the number of positive charges added to DNA is in excess of the number of negative charges from the

DNA.[42] Experimentally, this is represented as a molar ratio of nitrogen to DNA phosphate, or N/P charge ratio. Excess polycation (i.e high N/P ratios) is required for the formation of sufficiently small, stable nanoparticles for efficient cellular uptake. [43-45] The small size of these particles also allows for more efficient diffusion through intracellular and extracellular fluid.

The positively charged polyplexes are able to associate with the negative head groups of cellular membrane lipids, which helps to facilitate endocytosis.[42] Polyplexes are believed to enter the cells through three different endocytotic pathways: Clatherin-dependent endocytosis, the Caveolae pathway, and pinocytosis.[46] Once taken up into the cell through endosomes, polyplexes must be transported towards the nucleus. Fluorescence studies by Suh, et. Al. suggest that endosomes containing cationic polyplexes likely traffic near the nucleus by active transport along microtubules.[47]

The high positive charge density of the polymers contributes to the high buffer capacity, which is believed to be integral to polyplex release from endosomes for PEI and other cationic transfectors.[29, 48] Both Clatherin-dependent endocytosis and pinocytosis result in lysosomal degradation of endosomal contents.[46] The lysosomal pathway utilizes low pH along with degradative enzymes to break foreign materials along with recyclable cell components into their base biological molecules for use by the cell.[49] Additionally, one study by Gabrielson and Pack indicates that acidification also occurs in Caveolae derived endosomes, even though such vesicles are not destined for lysosomal degredation.[50] The mechanism by which cationic polyplexes are released from endosomes into the cytoplasm is still highly debated, but the most well accepted idea in the literature is known as the "proton-sponge hypothesis". According to this hypothesis, originally

proposed by Behr, the broad buffer capacity of PEI and PAMAM polyplexes resists acidification by proton pumps in endosomes.[5, 48] In response, proton pumps release more H^+ ions into the vesicles, leading to larger influx of counter-ions.[5] Osmotic swelling accompanies the increase in ion concentration, resulting in membrane rupture and release of polyplexes.[5, 51] Inhibition of endosomal acidification by drugs such as Bafilomycin and Nigericin lead to significant reductions in transfection efficiency, lending credibility to this idea.[34, 46] Additionally, microscopy studies have visualized endosomal burst in cells exposed to polycation/DNA complexes.[52]

While this mechanism has come to be accepted by many in the literature, a handful of studies call into question the validity of the "proton-sponge hypothesis". Banjaminsen et. al. used pH sensor nanoparticles co-localized to the lysosomes with fluorescently tagged PEI polyplexes to show that the pH of endosomes did not significantly change with the addition of PEI as would be expected if the concentration of PEI was high enough to cause endosomal burst by buffering.[53] Additionally, estimates of osmotic stress induced by polycation complexes by this buffering effect do not seem to indicate that endosomal burst is a realistic outcome.[51, 53] For this reason, it was suggested by Benjaminsen et al. that micron sized pore formation, as reported to be induced by surfactants in liposomes, may be another possible mechanism of endocytotic escape.[53-54] The presence of such pores in PEI transfections was observed by laser scanning microscopy by Bieber et. al. and have been proposed to be a source of the toxicity observed.[55-56]

Once DNA cargo have reached the cytoplasm, they must be transported through the nuclear membrane. The mechanisms underlying this process are very poorly characterized, and consensus on the pathway that polyplexes take is still to be reached. It is unclear

whether or not polyplexes travel through the nuclear membrane intact, or whether DNA must be released from polymer before transportation. The nuclear membrane is only wide enough for particles 30 nm or smaller to translocate through, which would preclude many cationic polyplexes based upon size alone.[57-58] A two colored Fluorescence correlation spectroscopy (FCS) study by Clamme et. al. did not indicate that bound polycation/DNA complexes existed within the nucleus during transfection, but did show that free polymer was present inside of the nucleus during transfection.[59] Both Clamme et. al. and Suh et. al. observed accumulation of PEI/DNA complexes was observed in the cytoplasm around the nucleus.[47, 59] Additionally, it has been suggested that transfection efficiency may be dependent upon cell cycle, with efficiency increasing during mitosis, when the nuclear membrane breaks down.[60] In fact, transfection studies of polymer and lipid transfections show higher efficiency in actively dividing cell cultures.[61-62] Alternatively, efforts have been made to add nuclear localization signals to genes of interest to increase nuclear uptake in non-dividing cell cultures, which are of interest for clinical applications.[60]

Whether it be intranuclear or perinuclear, several mechanisms for DNA release from polymer have been proposed. DNA release could be mediated by competitive binding of the cationic polymer with nucleic acids, most likely RNA, or other negative cell components.[63-64] Additionally, if the polyplex exists in the nucleus, Thomas and Klibanov have suggested that DNA could be stripped away from the polymer by the DNA polymerase complex, as has been observed to occur with histone bound DNA.[7, 65] Regardless of the mechanism of endosomal escape, cell transport, and nuclear translocation, it is clear that very few of the DNA molecules transfected end up in the nucleus, and the majority are degraded in the cytoplasm.[60]

While the positive charge of cationic DNA polyplexes confers characteristics that enhance transfection, it also comes with several drawbacks. Polyplexes can bind to cell structures, such as proteins and membranes, which can lead to cell death.[66-67] Additionally, in vivo, the positively charged polyplexes can bind to blood cells and negatively charged blood proteins, which lowers the efficiency of delivery.[17, 68-69] One study by Hong et. al. has shown that the high positive charge of polyplexes can lead to increases in permeability of membranes through pore formation, which in excess is deleterious for cells.[56]

A large number of factors, at times competing with one another, govern the effectiveness of cationic transfectors. An effective chemical agent must be capable of binding and condensation of DNA cargo, protection of payload from enzymatic degradation, and mediation of transport through the extracellular space into the cytoplasm and nucleus of the cell. However, the nucleic acids must not be so tightly bound that they are unable to be released and transcribed by the target cell, nor should the polyplex be harmful to cells or tissues. Development of better chemical transfectors, therefore, necessitates careful consideration of these factors that influence polymer/nucleic acid interactions.

1.4. Attempts to Optimize Gene Delivery

Because the commonly utilized commercial polymers, such as PEI and PAMAM, were not made to address the diverse barriers associated with gene delivery, great potential exists to modulate their chemical properties in order to better optimize ability to transfect.

As discussed above, successful gene delivery requires overcoming various energetic barriers. Often these barriers are in direct competition and therefore an optimization of these barriers is required. Because a high net positive charge is a common trait in chemical transfectors, many groups have studied the effects of charge reduction or modulation upon the efficiency of transfection. As described in the previous section, a high nitrogen to phosphate (N/P) ratio is necessary to condense polyplexes into stable nanoscale particles, and is important for endosomal escape into the cytoplasm, but can also be deleterious to cells and cause nonspecific interactions with components of blood and other tissues. Through reduction of the overall positive charge of the polymer, the affinity of DNA release may be modulated, as well as the extent of binding to negatively charged cellular components or blood/serum proteins. If an optimal charge density can be established, the limits of transfection efficiency and cytotoxicity of the base polymer may be improved in vitro and in vivo. There are several modes by which various groups have accomplished this goal. By grafting biocompatible and neutral groups such as polyethylene glycol (PEG) or dextran carbohydrate chains to PEI, several groups have noted a reduction in cytotoxicity and an increase in transfection efficiency over the base polymer.[16-19] Additionally, creation of tertiary complexes, by addition of an anion to polyplexes after complexation is believed to reduce cytotoxicity and nonspecific binding to proteins by reducing the positive charge on the outside of polyplexes, and through binding up free polycation in solution following preparation.[12-15] In addition to these two means of charge modulation, many groups have sought to reduce charge through covalent reaction of the positive amine groups. Acetylated branched PEI through creation of an amide bond on the primary and secondary amines was shown to decrease the binding affinity for DNA,

increase the intracellular release, and overall increase transfection efficiency up until a critical percent modification.[21-22] Other groups have shown PEI with covalently attached neutral zwitterions such as 2-methacryloyloxyethyl phosphorylcholine (PMPC) is both less cytotoxic and a more potent transfector than unmodifiedPEI, which is very similar to what was observed in PEG grafting onto PEI.[23-24] Additionally, work has been done by Lynn et. al. to create "charge-shifting" PEI derivatives that, when hydrolyzed over time, lead to an increase in negative charge along the polymer.[25] This approach has shown that a time based zwitterionic modulation of PEI can also lead to increases in transfection efficiency. The success of modification studies such as these indicate the potential for fine tuning the transfectibility of chemical agents by modulation of their positive charge, and suggest that further optimizations may lead to more viable chemical agents that are better able to compete with viral based methods.

Chapter 2: Synthesis and Characterization of Zwitterionic PEI

2.1. Introduction

While the high cationic charge of PEI lends itself towards high cytotoxicity and low serum stability; it also allows for the condensation, tight packaging, and endosomal escape necessary for gene expression.[5, 36, 55-56, 66-69] Not only must DNA be tightly packaged and protected from enzymatic degradation, but also must be released at an appropriate cellular location.[5, 7, 36-37] For this reason, a balance in the charge content of PEI through addition of zwitterionic character could lead to optimal transfection. Previous work by the DeRouchey group indicated that mixed charge peptides were able to condense DNA. Here, zwitterionic charge was introduced to 25 kDa branched polyethylenimine (bPEI) through addition of succinyl groups through post polymerization modification. In collaboration with the laboratory of Dr. Pack, a spectrum of succinylated PEI derivatives (zPEI) were created. This chapter will explore the relationship between percent modification of zPEI and the resulting binding and release properties of DNA with the polymer.

2.2. Materials and Methods

2.2.1. Materials

Branched 25 kDa PEI, succinic anhydride, hydrochloric acid (37%), solid sodium hydroxide, dextran sulfate, D_2O, and sodium azide were purchased from Sigma Aldrich (St. Louis, MO). Sodium Carbonate, 10 x phosphate buffered saline, ethidium bromide,

30% glycerol, 2k MWCO Slide-A-Lyzer dialysis cassettes, and 0.5 M EDTA were purchased from ThermoFisher Scientific (Waltham, MA). Sodium Bicarbonate was purchased from EM Science (Darmstadt, Germany). Tris-Acetate-EDTA buffer (TAE, 50x) was purchased from Omega Bio-tek (Norcross, GA). Tris HCL buffer was purchased from Madiatech, Inc (Manassas, VA). Plasmids pUC19 (1 mg/mL) and pUC18 (0.5 mg/mL) were purchased from New England Biolabs (Ipswich, MA) and ThermoFisher Scientific (Waltham, MA) respectively. DNA ladder (1 kB) was purchased from Fermentas Biotechnology (Waltham, MA). Solid Agarose I, 0.2 micron syringe filter units, and 1000 mL 0.2 micron PES vacuum filter units were purchased from VWR (Radnor, PA). Bromophenol Blue was purchased from Eastman Kodak (Rodchester, NY). All double distilled H2O used was purified through a dH20 – Milli-Q water purification system equipped with a 0.22 micron Millipak 40 sterile Millipore filter (Billerica, MA). Acetylated PEI received from Logan Warriner (UK Chemical and Materials Engineering, Laboratory of Dr. Dan Pack).

2.2.2. Synthesis and Characterization of zPEI

2.2.2.1 Synthesis and Purification of Succinylated PEI

Sodium bicarbonate buffer (0.1 M, pH 9) was prepared by mixing aqueous solutions of 0.1 M sodium carbonate and 0.1 M sodium bicarbonate. A half gram of 25 kDa branched PEI was dissolved in 3 mL of pH 9 bicarbonate buffer in a 7 mL scintillation vial. Once dissolved, solid stock of succinic anhydride was added and immediately mixed.

The amount of succinic anhydride was chosen based upon the intended molar ratio of substitution. Samples were magnet stirred and allowed to incubate at 60 °C for 4 hours. Following reaction, solutions were filtered through a 0.2 micron syringe filter. The resulting solutions were loaded into 2K MWCO Slide-A-Lyzer dialysis cassettes and allowed to equilibrate with double distilled water (ddH_2O) for 48 hours with constant replacement of the external water solution. After 48 hours, the solutions were emptied from the dialysis cassettes and frozen at -80 °C prior to lyophilization. Synthesis was performed by Logan Warriner (Chemical and Materials Engineering, University of Kentucky) and Joseph Duke (Chemistry, University of Kentucky).

2.2.2.2. H-NMR and FTIR Analysis

In order to evaluate the yield of the reaction and test for the presence of unwanted side reactions, H^1-NMR and FTIR spectra were taken on the succinylated PEI in addition to the unmodified branched PEI. For H-NMR, samples were dissolved at ~5-10 mg/mL in dH2O. Percent succinylation was estimated by Logan Warriner from H-NMR spectra taken on a 400 mHz Varian NMR spectrometer. NMR data processed and integrated using Agilent VnmrJ software. An iS50 FT-IR equipt with a diamond ATR was used to collect absorbance data from 4000-400 cm^{-1} radiation from spectrum on solid PEI stocks through OMNIC software (ThermoFisher Scientific; Waltham, MA). FTIR data was output as a CSV file for processing in Origin (OriginLab Corporation; Northampton, MA).

2.2.2.3. pH Titration

For each of the zPEI derivatives and the unmodified, 2 mg were dissolved into 5 mL of ddH_2O. The pH of each sample was adjusted to 11.5 using 1 M sodium hydroxide. Each solution was then titrated with 5 μL additions of 1 M HCl. Solutions were mixed well prior to pH measurement on an Accumet AB15 pH meter (Hudson, MA). Titrations were performed by Logan Warriner and Joseph Duke.

2.2.3. Characterization of DNA Polyplex Formation

2.2.3.1. Gel Retardation Assay

Agarose gel electrophoresis was utilized in order to assess DNA condensation efficiency of unmodified and modified (uPEI and zPEI, respectively). 200 ng of plasmid DNA (pUC19 or pUC18) were mixed with the desired weight ratios of PEI. Both DNA and plasmid was prepared in 10 mM Tris (pH 7.5), 400 μM NaN_3 buffer that was filtered before use with a 0.2 μm PES filter unit. All samples were brought up to a final volume of 12 μL by addition of Tris buffer, vortexed for ~1 minute, and allowed to incubate at room temperature for 45 minutes before loading the sample onto the gel. Following incubation, 2.4 μL of 6x loading dye was added to each sample and mixed. Ten μL of each PEI/DNA sample was pipetted into the wells of a 0.8% agarose gel and ran at 100 V for approximately 2 hours in 1xTAE buffer (40 mM Tris pH 8, 20 mM acetic acid, 1 mM EDTA, made from dilution of 50 x stock into ddH_20, passed through a 0.2 μm PES filter.

Samples were run next to a single well of 20 μg/mL solution of 10 kbase DNA ladder dissolved in 10mM tris. All agarose gels were prepared by dissolving agarose in 1x TAE buffer by microwave heating, and allowing to cool for at least 1 hour. Gels were stained for 45 minutes in a 200 μL solution of 0.5 μg/mL ethidium bromide dissolved in 1xTAE. Gels were subsequently destained for 30 minutes in 200 μL 1xTAE solution. A BioRad ChemiDoc MP Imaging System was used to image each gel through Image Lab software (BioRad; Hercules, Ca).

2.2.3.2. Polyplex stability in the presence of Dextran sulfate

In order to determine the stability of DNA/zPEI complexes, polyplexes of PEI/pDNA (0.2 ug pUC19) at fixed w/w ratio, chosen based upon the needs of the experiment as discussed below, were brought to a final volume of 5 μL in 10 mM tris buffer and incubated for 45 minutes at room temperature. The desired weight ratio of a competitor polyanion, here dextran sulfate (DS) in 10 mM Tris, was then added to the samples to induce DNA release. All DS/PEI/pDNA samples were then brought to a final solution volume of 12 μL by addition of 10 mM Tris. Samples were then vortexed and incubated for 30 minutes. 2.4 μL of 6x loading buffer and preparing and running 0.8% agarose gel as described above. A BioRad ChemiDoc MP Imaging System was used to image each gel through Image Lab software.

2.2.3.3. DLS Zeta Potential Characterization

Polyplex solutions were formed by preparing a 0.02 mg/mL solution of pBR3 plasmid in 0.1 x PBS. Polymer solutions dissolved in 0.1xPBS at appropriate concentrations for the desired weight ratio of polymer to plasmid were added dropwise to the DNA solution while being mixed. Samples were well mixed and left to incubate at room temperature for 30 minutes. Polyplex solutions were diluted to 1 μg/mL in 0.1xPBS prior to measurement. A Zetasizer Nano ZS (Malvern Instruments; Malvern, UK) was used to collect all DLS and Zeta potential measurements. All DLS and Zeta Potential measurements and sample preperations performed by Logan Warriner.

2.3. Results and Discussion

2.3.1. Characterization of Synthetic Product

2.3.1.1. Spectroscopic Analysis of zPEI

In order to probe the effect of increased zwitterionic character upon the ability of the commercial transfecting agent polyethylenimine (bPEI) to condense DNA, a series of zwitterionic PEI derivatives (zPEI) were synthesized through post-polymerization modification via succinylation of primary and secondary amines as depicted in Figure 2.1.

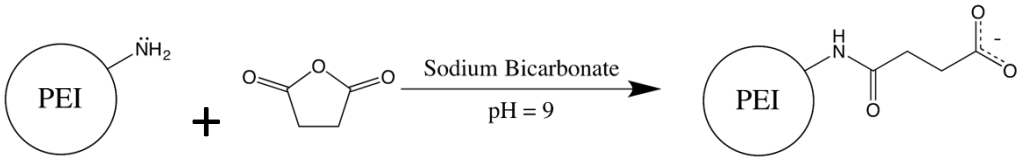

Figure 2.1. Reaction scheme for the synthesis of succinylated PEI (zPEI) using succinic anhydride. Reaction is also possible with secondary amines, but for simplicity, only substitution upon primary amines are shown.

zPEI with percent modification ranging from 5-35% were synthesized by reaction of commercially available, 25kDa branched PEI dissolved in 0.1M bicarbonate buffer (pH 9) with succinic anhydride. Branched PEI is contains a mix of primary/secondary/tertiary amines, broadly thought to have a ratio of 25/50/25.[28] The variant used in this work, 25 kDa bPEI, has been reported by Sigma Aldrich to contain an amine content of roughly 31% primary, 39% secondary, and 30% tertiary amines. By varying the SA:PEI ratio in the reaction mixture, polymers with varying degrees of modification are obtained through reaction with primary and secondary amines. By adjusting the pH to 9 with bicarbonate buffer, we expected to improve yield of succinylation by deprotonating the PEI amines increasing the nucleophilicity of the amine nitrogen. bPEI and succinic anhydride were mixed and allowed to react for 4 hours. Following the succinylation, zPEI samples were dialysized to remove residual succinic anhydride and freeze-dried.

Total percent of amines reacted was characterized via H^1-NMR by Logan Warriner by division of the integration of peaks representing the succinyl methylene at δ 2.3-2.5 by those representing the PEI ethylene backbone at δ 2.6-3.34. H^1-NMR characterization

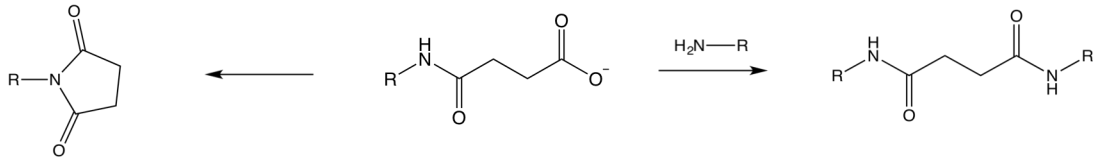

Figure 2.2. Potential side reactions, including succinimide group formation (left) and crosslinking between amines (right).

revealed percent substitutions of 5.8, 8.0, 15.4, 26.7, and 35.0% of total amines reacted for the 5 different PEI derivatives reacted and purified. A previous paper focused on siRNA delivery by Zintchenko et al. performed succinylation of PEI but saw a maximum of 20% amine groups reacted when the reaction was performed in pH 5 solution of water and DMSO.[20] siRNA knockdown was then examined but only at the one percent modification.[20]

In order to ensure that the succinylation of bPEI was the primary product, FTIR was used to characterize the functional groups of our post-polymerization succinylation. Because different bond types have bending and stretching modes with frequencies on the order of infrared (IR) radiation, IR absorption spectra of a sample can be used to identify functional groups of interest.[70] Of concern was the potential for unintended side reactions, namely crosslinking or ring closure to form a succinimide group (figure 2.2). Both formation of succinimides and crosslinking, either via intra- or inter-molecular nitrogen, would reduce the overall charge at neutral pH by replacement of amine groups with amide groups with reduced pKa values, in contrast to the production of zwitterionic character that was intended. Inter-molecular crosslinking would lead to larger molecular weight branched PEI derivatives, which would also confound the effects of charge modulation.

The resulting IR absorbance spectrum of our 5 zwitterionic derivatives of branched PEI, along with the unmodified, are depicted in figure 2.3 below. In unmodified PEI, two peaks at ~2934 cm^{-1} and ~2815 cm^{-1} indicate the presence of C-H stretches corresponding

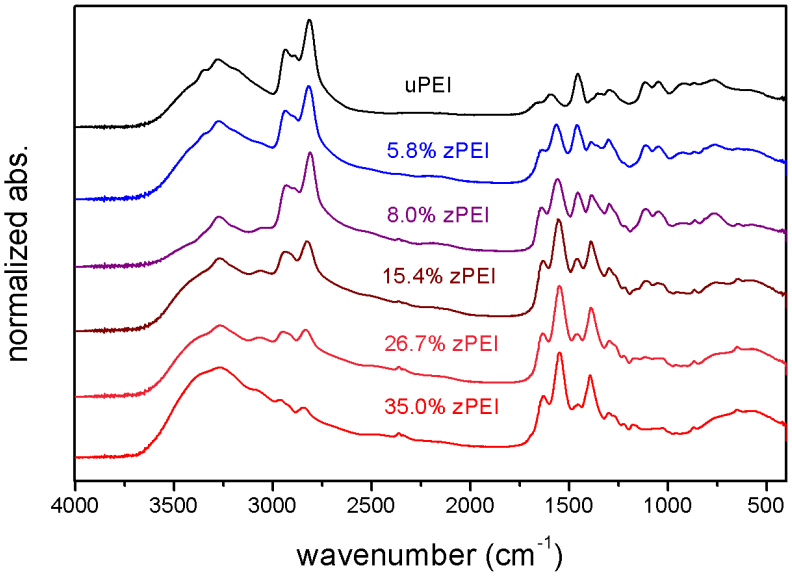

Figure 2.3. FTIR Analysis of Succinylated bPEI Derivatives

to the ethyl groups present in PEI. The peaks at ~3349 cm^{-1} and ~3270 cm^{-1} indicate the N-H stretch of primary and secondary amines. As the percent modification increases, the first of these peaks is diminished in intensity, indicating the disappearance of primary amines. The two peaks at 1592 cm^{-1} and 1456 cm^{-1} correspond to the N-H and C-H bends in the amine and ethyl groups respectively. As percent succinylation increases, bands appear at 1629 cm^{-1} and 1548 cm^{-1} indicating the presence of a C=O stretch in the amide bonds and carboxylate groups created, and at 1393 cm^{-1} indicating C-O stretches in the carboxylate of the succinyl group added. A broad peak appears between 3500 and 3000 cm^{-1}, which is likely due to the presence of an O-H bend on the succinyl group COOH, but could also represent hydrogen bonding between succinyl groups and PEI amines. A sharp

peak at ~1750 cm^{-1} indicating the C=O stretch of a succinimide group was not detected in any of the spectra taken, which is evidence against succinimide formation as a side reaction. It is difficult to say whether or not crosslinking is evident from the spectroscopic analysis performed, but high molecular weight inter-molecularly crosslinked products are likely to be largely eliminated by the filtration of products following synthesis. During synthesis, insoluble precipitation was observed, likely high molecular weight crosslinked PEI, but filtration through a 0.2 micron pore size was used to remove precipitants prior to dialysis and lyophilization. Zeta potential and gel electrophoretic data later discussed in sections 2.2.2 indicate the presence of negative charge in addition to the reduction of positive charge, likely meaning that if side reactions were present, they did not entirely remove the added negative charge of the succinyl groups.

2.3.1.2. Effect of Percent Succinylation on Buffering Capacity of zPEI

As described in chapter one, the buffering capacity of polycations is not only indicative of the charge density due to amine groups, but also has been proposed to influence the mechanism that polyplexes are able to escape the endosomal compartments in target cells. To better characterize the effect of succinylation upon the buffering capacity, titrations on 0.4 mg/mL solutions of our modified zPEIs, along with unmodified PEI and water. The ability of zPEI to buffer aqueous solutions is related to the amine, amide, and carboxylic content of the modified polymers. As previously described in section 1.2, the amine groups of PEI possess a wide range of pKa, beginning at 9.98 and

decreasing as protonation of amines increases. [22, 29] Carboxylic groups typically buffer at much lower pH, having pKa ~ 4. Additionally, amides buffer at a pH of ~ 0. Therefore, the buffering capacity of zPEI should be proportional to the substitution ratios, as characterized by H-NMR. The titration curves are shown in figure 2.4. As percent substitution increases, the titration curves shift to the left, indicative of a reduction in ability of the polymers to buffer over the pH range tested.

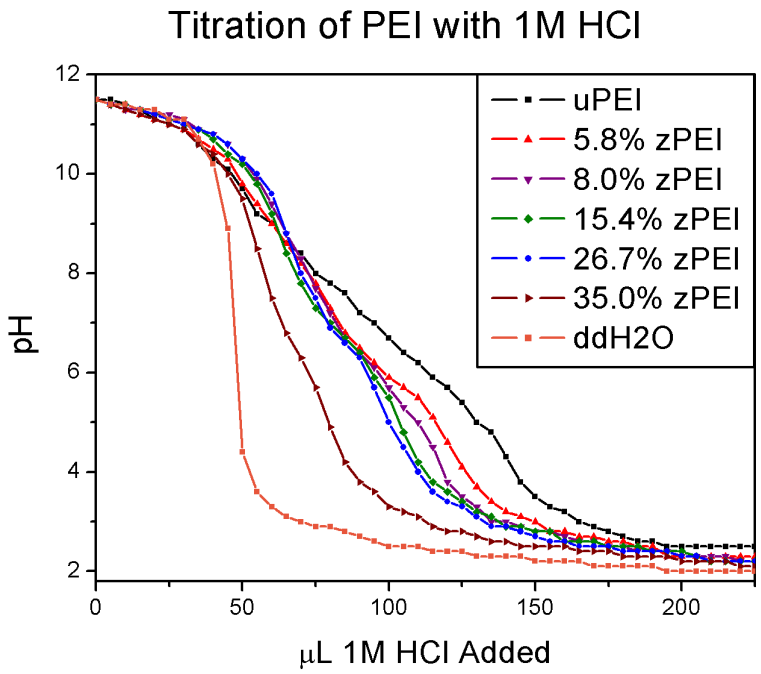

Figure 2.4 Titration of zPEI Derivatives with HCl. Prior to measurement, all samples titrated to a pH of 11.5.

Extent of buffering capacity was estimated as the number of μmol of HCl necessary to shift the pH of the PEI solutions from 7.4 to 4. This ph range was chosen because it is the relevant range of buffering between extracellular pH and the acidic pH of endosomal

compartments. Table 2.1 below shows the buffering capacities of zPEI as compared with the unmodified and water. Buffering capacity was calculated as follows:

$$\beta = \frac{\mu mol_{HCl}}{|\Delta pH|(V_{buffer})} \quad \text{(Equation 2.1)}$$

The buffer capacity, β, is expressed in terms of μmol strong acid per L buffer solution. For all but between 8.0% and 15.4% substituted zPEI, the buffering capacity between pH 7.4 and 4.0 decreases as percent substitution increases. It is likely that no difference in buffering capacity between 8.0 % and 15.4 % zPEI was detected because of the simplicity of the calculation in addition to limitations in resolution of our titration.

Table 2.1 Extent of buffering of succinylated bPEI derivatives

Sample	Buffering Capacity ($\mu mol_{H^+}/mL_{buffer}$)
uPEI	3.53
5.8% zPEI	3.24
8.0% zPEI	2.35
15.4% zPEI	2.35
26.7% zPEI	2.06
35% zPEI	1.76
ddH_2O	0.59

2.3.2. Characterization of Complex Formation and Dissociation

2.3.2.1. Complex Formation and Dissociation of zPEI

Agarose gel electrophoresis was used to characterize the binding affinity and polyplex stability of our zPEI/DNA and uPEI/DNA polyplex nanoparticles. For all percent

modification, DNA migration in the gel is markedly retarded with increasing uPEI or zPEI concentration, showing that all PEIs investigated are capable of condensing DNA. We hypothesize that both polyplex condensation and complex stability will be highly dependent on the percent succinylation in the zPEI samples.

In agarose gel electrophoresis, a current is passed through an electrolyte containing solution through a polymerized gel. DNA samples are negatively charged, so when exposed to an electric current, DNA will migrate away from the negative cathode and towards the positive anode. Due to steric constraints when diffusing through the polymerized agarose it was loaded, smaller DNA molecules will diffuse more quickly than larger ones. For this reason, agarose gel electrophoresis can be used to separate and visualize molecules both by charge and mass. A simple schematic of an agarose gel setup is shown below in figure 2.5a. DNA containing agarose gels are often stained with ethidium bromide, and intercalating agent, in order to fluorescently image the location of DNA bands following running of the gel. In figure 2.5b, a typical agarose gel image of pUC19, a 2686 base pair containing plasmid, is shown. The supercoiled, or tightly wound and compacted variant of the plasmid is labelled s, and it diffuses further than the band labelled n and l, representing the nicked open coiled and linear conformation of the plasmid, respectively. The presence of damaged plasmid (bands n and l) in the commercial plasmid is a result of the method of synthesis and purification of the DNA.

Gel retardation assay was used to visualize the disappearance of plasmid DNA bands with increasing amounts of polymer to quantify the relative affinity of zPEI for

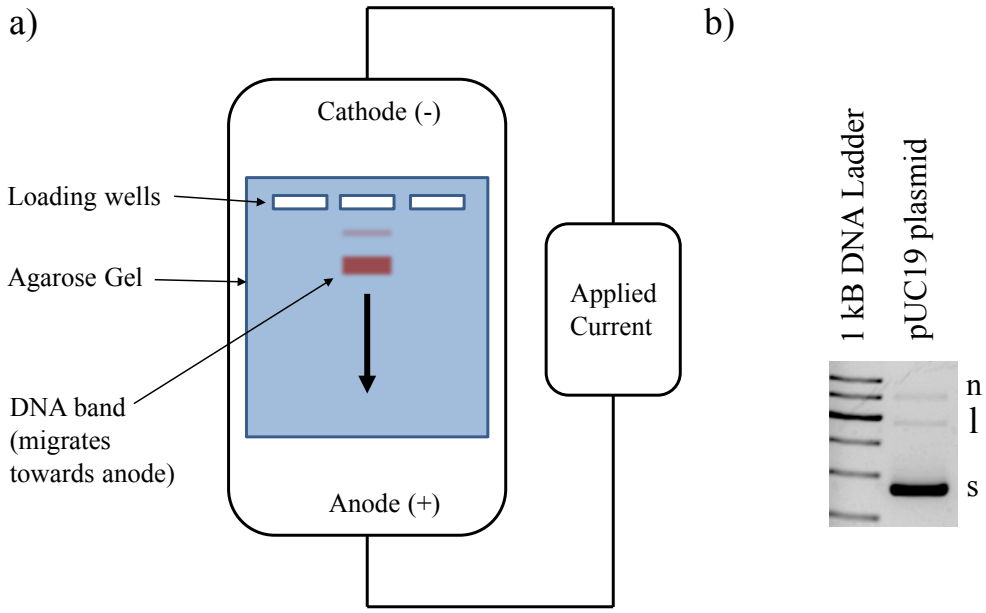

Figure 2.5. a) simple schematic of agarose gel electrophoretic on plasmid DNA. b) representative gel bands of the supercoiled (s), nicked open coiled (n), and linear variants (l) of pUC19 plasmid next to a 1 kB DNA ladder

binding DNA. As the amount of polymer added to DNA increases, the amount of free DNA in solution will decrease. When run in a gel with progressively increasing amounts of polymer, the effect will be a disappearance, and in some cases a smearing, of the DNA bands. DNA polyplexes gain positive charge, and are unable to migrate towards the positive anode. For this reason, bound DNA either becomes entrapped in the loading wells, or diffuses towards the negative cathode, out of the gel. Smearing is presumably observed due to the presence of noncondensed DNA molecules which are still interacting in some manner with the polycation thus retarding the DNA migration.

Shown in Figure 2.6, is the gel retardation assay of 0.2 µg pUC19 with varying weight ratios of uPEI and zPEI. The plasmid DNA exists primarily in the supercoiled form. For uPEI, complete condensation was observed by electrophoresis at weight ratios of 2 (N/P = 15.4) as visualized by the complete disappearance of the supercoiled band in the gel in Fig. 2.6A. As anticipated, more zPEI was required for complete condensation with increasing percent modification. A weight ratio of approximately 6 is necessary to visualize disappearance of DNA bands in 35.0% succinylated PEI (Fig 2.6F). There is some ambiguity between 8.0% and 15.4% succinylated PEI which may suggest imperfections in our H-NMR characterization (Fig. 2.6C-D). It is also possible that different substitution ratios differ in the numbers of primary and secondary amines that reacted to form succinyl groups. Differences in the location and distribution of charge on the surface of the polymer, or on the inside could lead to varying properties of complexation with DNA. These results reveal that the zPEI samples examined were able to condense plasmid DNA. However, with increasing percent succinylation, more zPEI was required to fully condense the DNA.

Polyplex stability was also examined using a gel shift assay. Through the addition of a polyanion competitor, polyplex DNA can be released and visualized by gel electrophoresis. The amounts of competitor required to release DNA is then directly related to the stability of the complex. Here, we have used dextran sulfate (DS) as our competitor polyanion. DS was found to be both cheaper and more effective in DNA release compared to another commonly used competitor, heparin sulfate. uPEI and zPEI polyplexes were formed as discussed previously. Since the highest required weight ratio for 35% zPEI/DNA was observed to be 6 (Fig 2.6); all DNA release assays were performed

at this weight ratio. DNA release assays upon addition of DS is shown in Figure 2.7uPEI shows complete release after a weight ratio of 10 DS to DNA. zPEI shows release is dependent on the degree of succinylation in the condensing agent. For zPEI, less competing

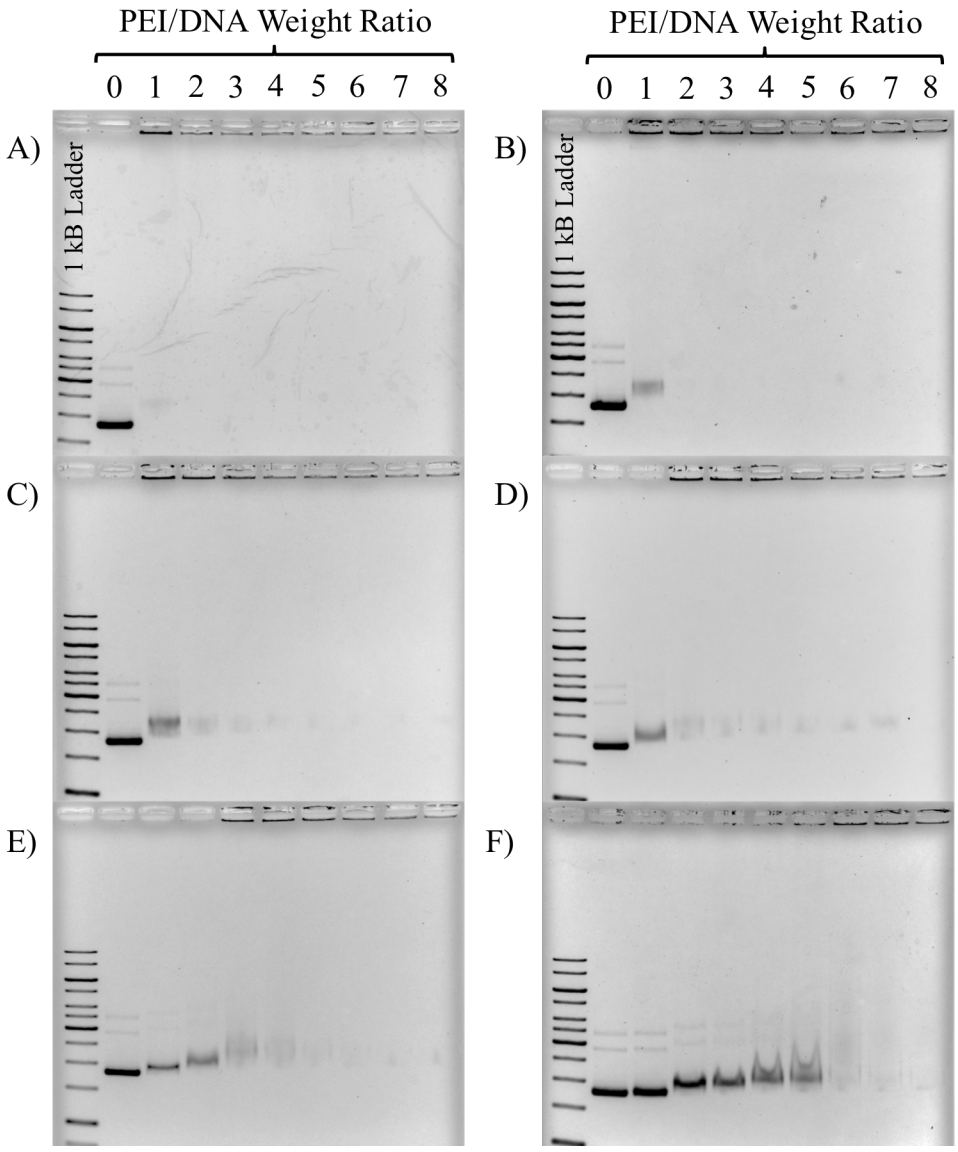

Figure 2.6. Gel retardation assay of zPEI complexation with pUC19 plasmid. A) Unmodified bPEI B) 5.8% zPEI C) 8.0% zPEI D) 15.4% zPEI E) 26.7% zPEI F) 35.0% zPEI

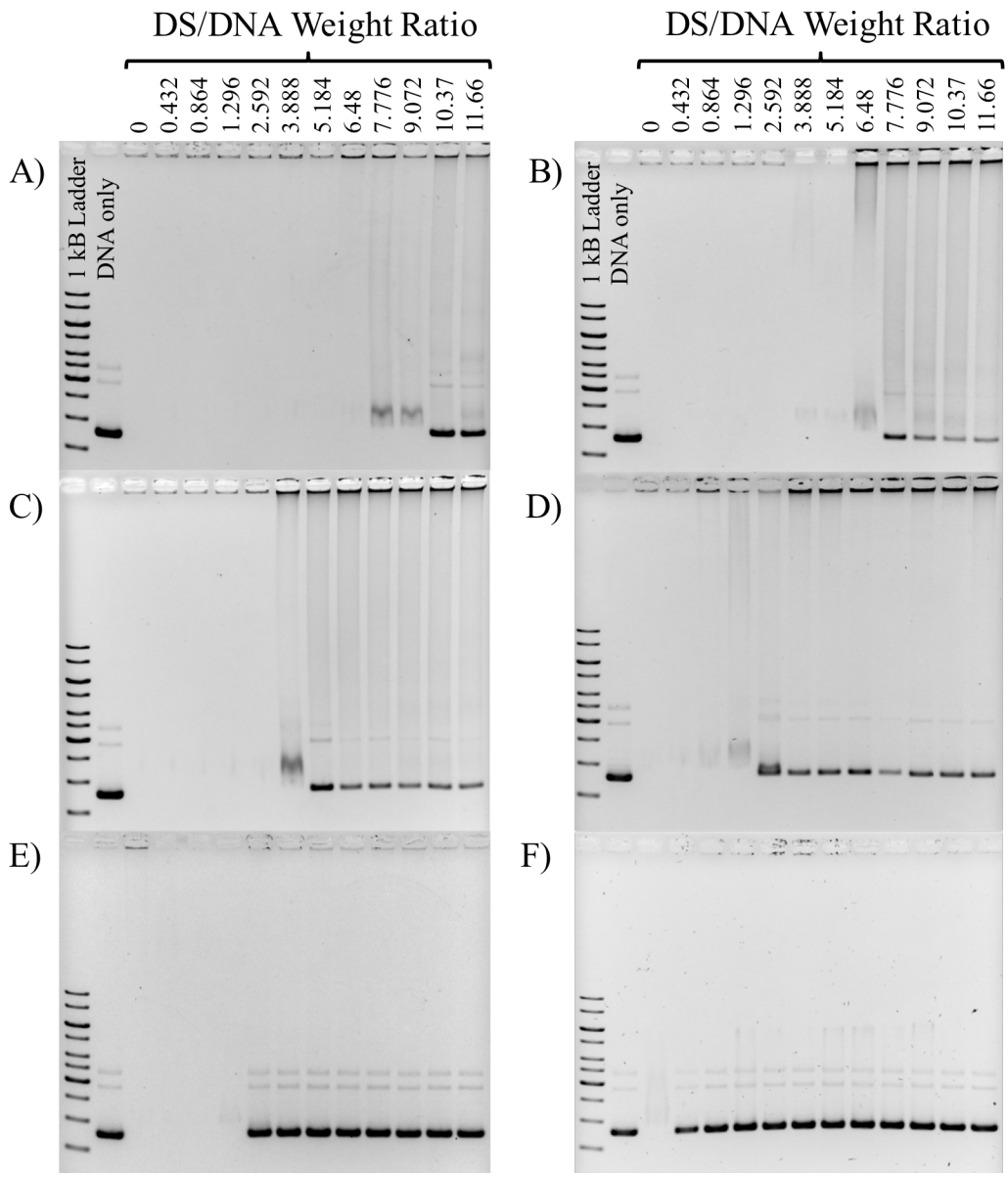

Figure 2.7. Dextran Sulfate Release Assay of zPEI complexation with pUC19 plasmid. Complexes formed at weight ratio PEI/DNA of 6. A) Unmodified bPEI B) 5.8% zPEI C) 8.0% zPEI D) 15.4% zPEI D) 26.7% zPEI E) 35.0% zPEI

polyanion (DS) is required to release DNA with increasing percent modification of the PEI. Like the previous figure, there is some ambiguity between 15.4% zPEI and 26.7% zPEI, which seem to show the opposite trend in Figure 2.7. In a similar fashion to what was seen with the binding gels of zPEI, this may suggest inadequacies in our current methods of characterization between these two polymers. In particular, it is possible that the 15.4% zPEI contains a different ratio of substituted primary and secondary amines.

The colloidal properties were also investigated for these polyplexes using dynamic light scattering (DLS) and Zeta potential measurements to characterize the size and charge of zPEI/DNA polyplex nanoparticles. DLS correlates the scattering of light off of particles in solution with Brownian motion in order to measure the magnitude and variance of the hydrodynamic radius of molecules.[71] Zeta potential analysis correlates the Doppler shift in frequency of scattered light off of particles in solution under an applied current from an electrode.[72] This allows for quantification of a "zeta potential" (mV) which is directly related to the sign and magnitude of particle surface charge.[72] Polyplexes were prepared at a PEI/DNA weight ratio corresponding to the optimal conditions for transfection, as established in HeLa cell cultured performed by the Pack laboratory.[73] The measured values for radius and zeta potential are shown below in table 2.2. No clear trend was evidenced from this data as a function of the degree of modification. All particles, except for the 26.7% zPEI, had radii under 300 nm, indicating that zPEI molecules are still suitable for cell uptake in delivery applications. The radii of zPEI are larger in scale than the unmodified polymer, likely due to the reduction in positive charge density in DNA/PEI

particles, which reduces the electrostatic repulsion between molecules. The zeta potential of all zPEI derivatives, except for 35% zPEI, remained cationic. Only 35% zPEI shows a

Table 2.2 DLS and Zeta Potential Measurement of zPEI Derivatives

Sample	Radius (nm)	Zeta Potential (mV)	Optimal w/w PEI/DNA*
uPEI	61.3 ± 10.3	15.1 ± 2.0	1
5.8% zPEI	174.4 ± 9.68	15.0 ± 1.8	2
8.0% zPEI	286.6 ± 2.8	11.9 ± 2.1	4
15.4% zPEI	205.3 ± 2.8	9.62 ± 1.2	4
26.7% zPEI	669.8 ± 37.76	11.8 ± 1.8	4
35% zPEI	139.6 ± 14.6	-1.3 ± 1.4	4

* Determined by Logan Warriner (Chemical and Materials Engineering) by HeLa transfection

charge reversal resulting in an observed negative zeta potential. We hypothesize that as positive amine groups are removed by succinylation, neighboring unreacted amine groups pKa groups are likely to shift upwards, so that even as amines are removed, and negative succinyl groups are added, the charge of PEI at physiological pH is able to remain net positive. Only in the 35% substituted zPEI, did the addition of negative charge overwhelm the positive charge of the polyplex. This is similar to what was observed in acetylated PEI derivatives by Gabrielson, et al. where acetylated PEI derivatives were able to condense DNA with positive charge and radii below 300 nm.[22] It is likely that the large particle sizes observed in the 26.7% zPEI and negative potential in the 35.0% zPEI are due to the addition of zwitterionic character, in contrast to just the removal of amine groups in acetylation. It is surprising that particle formation between 35% zPEI and DNA only

produces particles of around 140 nm, even though the net charge on the polyplexes is negative.

2.3.2.2. Comparison of binding and release properties of a charge neutral modification

Modulation of polymer/DNA interactions by replacement of positive charge with charge neutral groups has proven to improve the transfectability of cationic polymers. In particular, the Pack group have shown that the acetylation of PEI can increase the transfection efficiency of PEI by 58 fold.[21-22] A simple schematic of this reaction is illustrated below in figure 2.8. In order to compare the effect of addition of charge neutral

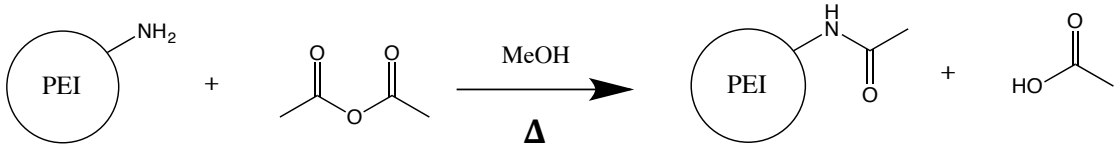

Figure 2.8 Reaction scheme for the synthesis of acetylated PEI using acetic anhydride. Reaction is also possible with secondary amines, but for simplicity, only substitution upon primary amines are shown.

groups to our zwitterionic modification, identical binding and release agarose gel assays were run on acetylated PEI (acPEI). Several substitution ratios of acetylated PEI (33.0%, 57.1%, and 93.1%) were provided by the Pack lab and synthesized and characterized as previously reported.[21-22] Acetylation is very similar to the succinylation of zPEI, but

instead of replacing the positively charged amine group of PEI with a negative succinyl group, it is replaced with a neutral acetyl group.

The binding gels for acPEI are displayed in figure 2.9 below. A polymer to DNA weight ratio of 1.75 is required to visualize the complete binding up of pUC19 by 17.1% acPEI, and a weight ratio of 2.5 is necessary to see complete binding by 37.4% acPEI. The release gels of acetylated PEI are displayed below in figure 2.10. As acetylation increases, the amount of dextran sulfate required to cause the full release of DNA also increases.

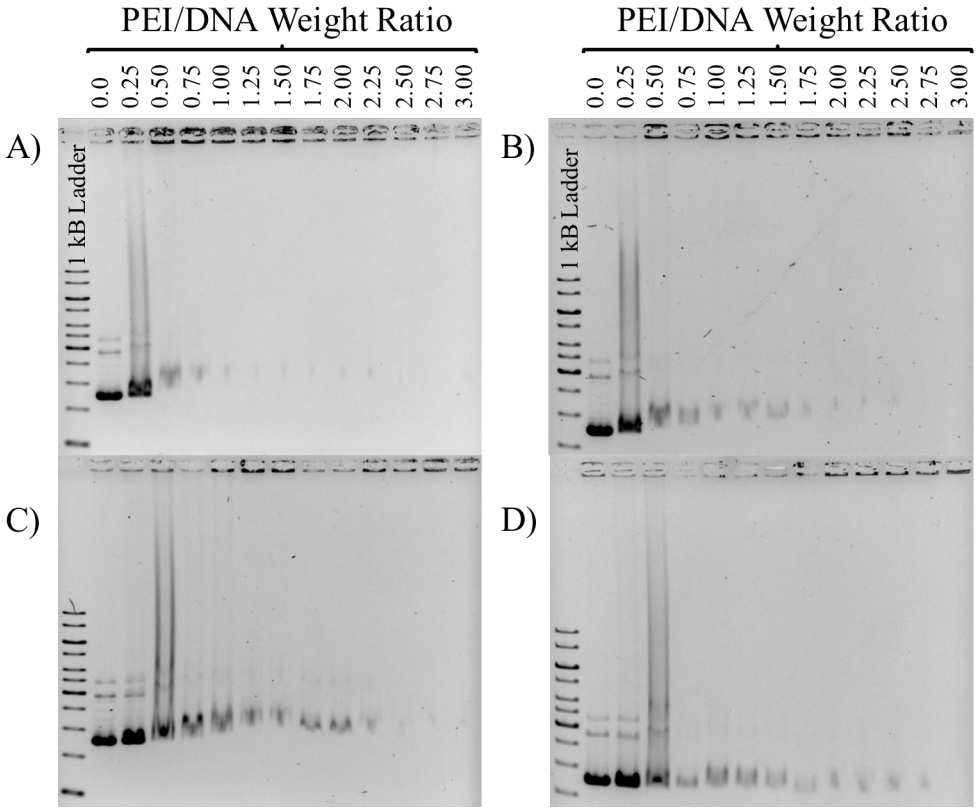

Figure 2.9. Gel retardation Assay of acPEI complexation with pUC19 plasmid. A) Unmodified bPEI B) 17.1% acPEI C) 37.4% acPEI D) 68.4% acPEI

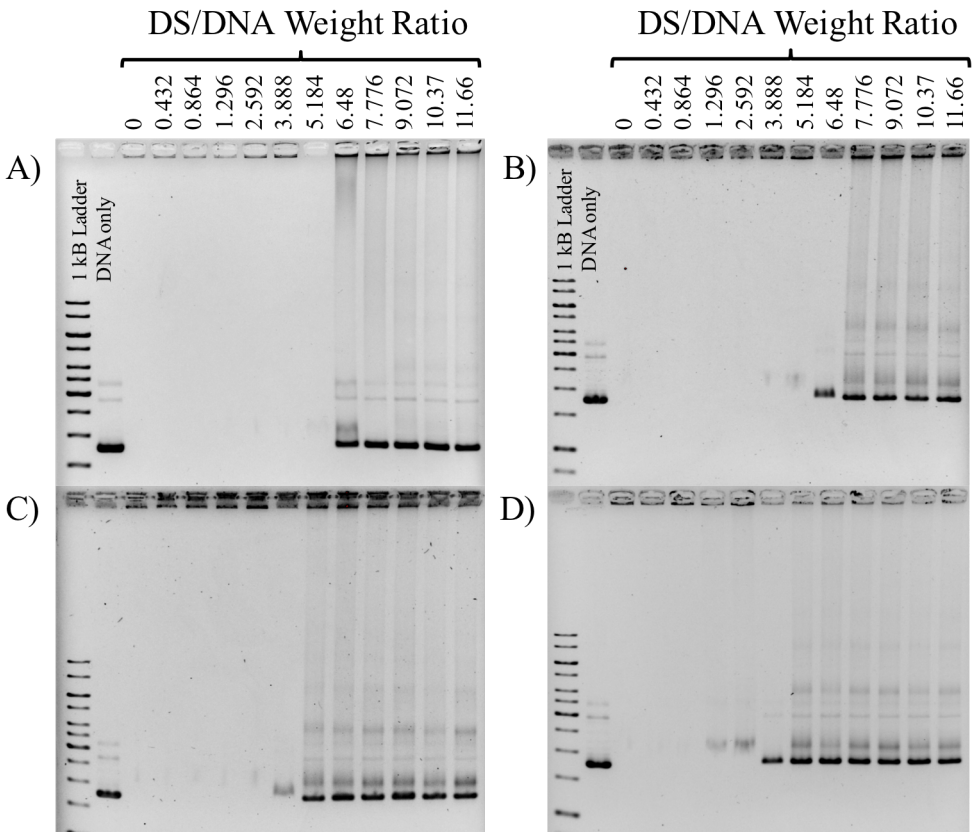

Figure 2.10. Dextran Sulfate Release Assay of acPEI complexation with pUC19 plasmid at a PEI/DNA weight ratio of 6. A) Unmodified bPEI B) 17.1% acPEI C) 37.4% acPEI D) 68.4% acPEI

In contrast to zPEI, acPEI condenses pDNA fully at much lower weight ratios suggesting a higher affinity for binding. For example, 37.4% acetylated PEI required a weight ratio of 2.5 to completely condense pUC19 compared to nearly double this amount to fully condense the plasmid with the comparable 35% zPEI. In addition, the stability of the acPEI/DNA complex is also higher requiring significantly more dextran sulfate to

release the DNA. The release of 17.1% acPEI occurs at a DS/DNA ratio of 7.8, which is roughly double the weight ratio of DS required to release 15.4% zPEI. This effect is even more obvious for higher degrees of modification. 37.4% acPEI/DNA requires roughly 10 fold more dextran sulfate to release DNA compared to 35% zPEI/DNA. Taken together, this data suggests that succinylation represents a more potent method of modulating DNA binding and release character than acetylation.

2.3.2.3. zPEI leads to improved transfectibility and lowered cytotoxicity in HeLa cells

Transfection studies in HeLa cells, performed by the Pack lab, revealed that not only do low percent modified zPEI (5.8%, 8%, and 15.4%) lead to higher transfection efficiencies in a serum-free transfection environment, but zPEI is able to achieve efficiencies exceeding the unmodified polymer in serum.[73] Surprisingly, 5.8% modified zPEI in-serum is able to outperform the efficiency of transfection of uPEI in a serum-free environment, a rarely seen trait with chemical transfectors. These results have been replicated in other cell lines including MC3T3-E1 (mouse preosteoblast) and MDA-MB-231 (basal like breast cancer cell) where weight ratios were varied to determine an optimal transfection weight ratio. In order to better understand how succinylated PEI leads to higher transfection efficiencies, dextran sulfate release gels were run on each zPEI system at their optimal transfection weight ratios (serum-free HeLa transfection) with respect to DNA. The results are shown below in figure 2.11.

Interestingly, the release character for each of the polymers was somewhat similar. This suggests that affinity for release is quite alike at the optimal conditions for each zPEI. By adding more or less polymer, the release point of DNA can be tuned, and by adding

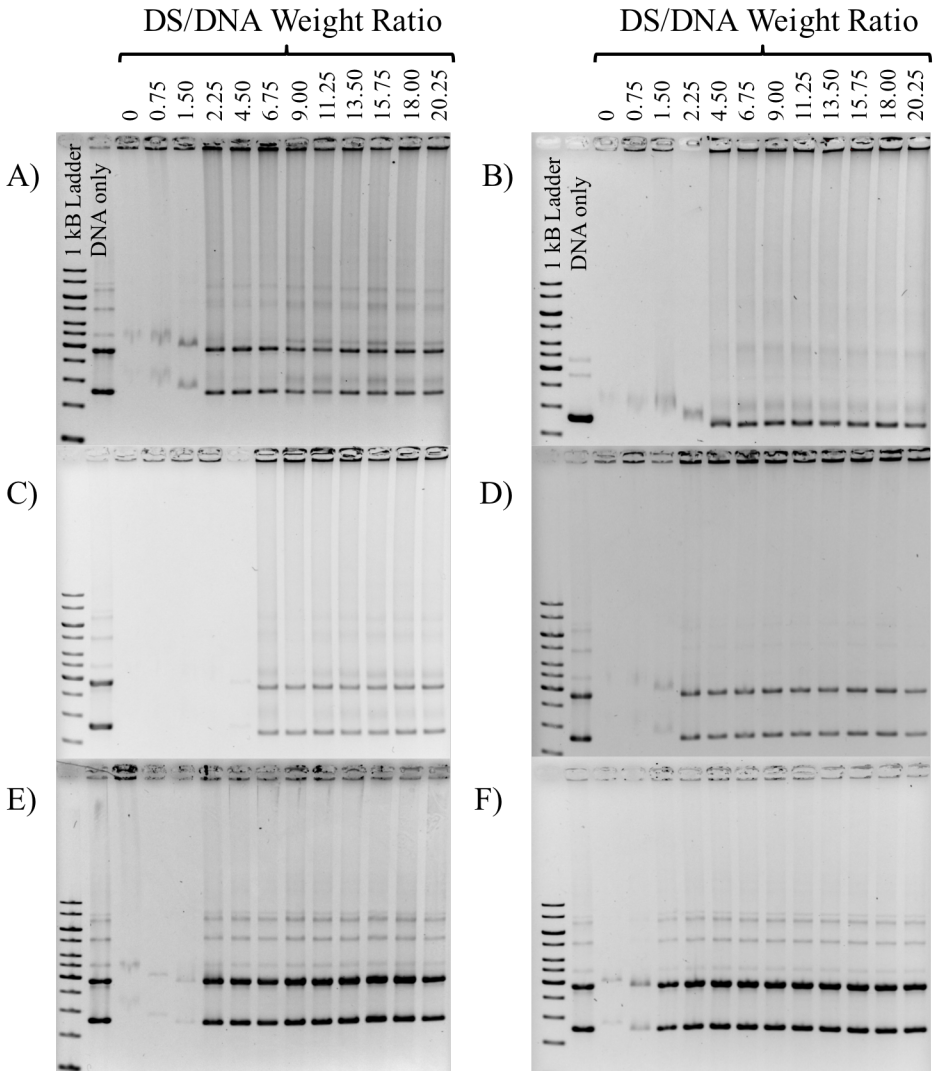

Figure 2.11. Dextran Sulfate Release Assay of zPEI complexation with pUC19 plasmid. Complexes formed at weight ratio PEI/DNA corresponding to the optimal transfection efficiency (Determined by Logan Warriner). A) Unmodified bPEI (w/w 1) B) 5.8% zPEI (w/w 2) C) 8.0% zPEI (w/w 4) D) 15.4% zPEI D) 26.7% zPEI (w/w 4) E) 35.0% zPEI (w/w 4).

zwitterionic character, the release point can be maintained while modulating other behaviors of the polymer, such as cytotoxicity or binding to serum components. Cytotoxicity studies by the Pack lab reveal that increasing zwitterionic character leads to a reduction in cell death when polymer is added to cells.[73] This, in addition to the in-serum transfections that showed superior efficiency compared to the unmodified indicate that these polymers are able to be modified without losing DNA binding affinity at optimal conditions. The derivative with the largest deviation from the release point of the unmodified was 5.8% zPEI. This also happened to be the transfection agent with the highest efficiency both in and out of serum.[73] Out of serum, this polymer performed roughly 5–fold better in transfection efficiency at a w/w ratio of 2 compared to the unmodified at its optimal w/w of 1.[73] Additionally, large improvements in efficiency were seen using in-serum transfection conditions. It is possible that this derivative, which holds DNA more tightly than the unmodified at its optimal weight ratio for out of serum transfections, reached a more ideal balance of binding character to cytotoxicity and resistance to nonspecific binding.

2.4. Conclusions

We report here a post polymerization reaction on branched PEI through succinylation with succinic anhydride. Our spectroscopic analysis, in combination with titration data and zeta potential analysis, confirm the creation of an array of succinylated zwitterionic "zPEI". We have shown that zPEI is capable of binding and condensing DNA,

forming stable nanometer scale colloidal particles, which are then capable of efficient cell transfection. Percent modification is correlated with a loosening of charge based interaction between DNA and the polymer, affecting both affinity for binding in addition to extent of release. Zwitterionic modification has been shown to modulate charge based interactions more aggressively than a similar acetylation reaction (acPEI), requiring lower substitution ratios to observe a similar effect upon particle formation and dissociation. These findings, in accordance with cell work performed by our collaborators in the Pack lab, suggests that charge reduction, along with addition of zwitterionic character, represents pathways towards creation of improved chemical gene delivery agents.

Future work need focus on better characterization and modulation of substitutions onto polymer amine groups. Since PEI is made up of primary, secondary, and tertiary amines, all distributed in different environments within the branched polymer structure, understanding to what extent different amine types are substituted on will contribute to a holistic understanding of the effects of post polymerization modification upon DNA interaction properties. In addition, it may be possible to tune reaction conditions to favor substitution upon different PEI amine groups, whether they be internal vs. external, or primary vs secondary amines. Biophysical, along with cellular characterization of polyplexes made up of varying amine containing PEI derivatives will further the understanding of a structure function relationship in cationic transfection agents.

Chapter 3: Analysis of Internal Structure of zPEI/DNA Complexes by Small Angle X-ray Scattering

3.1. Introduction

Chemical transfection agents, such as branched polymer polyethylenimine, have emerged as strong candidates for use in non-viral gene delivery due to their readily modular chemical properties in addition to a lower risk for immunogenicity. Previous literature has shown that chemical modification of PEI, such as PEGylation, alkylation, or the use of ternary polyanion/Polycation/DNA complexes, lead to reduced cytotoxicity in addition to improved transfection in cell cultures.[12-25] We have recently shown that the addition of zwitterionic charge through succinylation of the amine groups of branched polyethylenimine leads to altered binding and release properties of DNA (chapter 2). Cell work in collaboration with the Pack lab has revealed both a reduction in cytotoxicity and an improvement in transfection efficiency upon succinylation for zPEI compared to unmodified PEI (uPEI) both in and out of serum.[73]

While chemical modifications in polyplex formulations has often been shown to correlate to improved transfection efficiencies, presumably to altered DNA binding behavior, the effects of such changes upon the internal structure of polymer/DNA complexes has not been well established. Design of more efficient materials requires better understanding of both polymer-NA interactions and how the internal structures in polyplex nanoparticles relates to intracellular trafficking and gene delivery efficiency. In this study, we use small angle x-ray scattering (SAXS) to characterize the effect of succinylation on zPEI/DNA polyplex formation and structure. Because X-ray radiation lies between 0.01-

100 angstroms, X-ray based techniques are often chosen to study structural information on condensed molecular systems such as crystals with characteristic distances on the scale of angstroms.[74-75] SAXS is a variant of X-ray scattering used to study structural properties greater than 10 angstroms.[74, 76] Spacing between crystal or semi-crystalline planes can be determined, and in many cases molecular spacing as well as organization structure may be elucidated.[76] SAXS shows great flexibility with respect to sample preparation, as the sample analyzed need not be a true crystal, and can be powders, liquids, or DNA suspensions such as those studied in this work.[74, 76-77] Previous studies have shown mixtures of DNA and polycations ($\geq +3$), typical leads to self-assembly of the DNA helixes into a hexagonal lattice (representative image in figure 3.1 below).[77] These DNA helices are not touching, but rather separated by 5-15 Å of water. The DeRouchey lab, and others, have shown that the interaxial DNA spacings inside the condensates are highly dependent on cation chemistry. In this Chapter, we use SAXS to determine the DNA packaging as a function of percent zwitterion modification in zPEI/DNA and compare it to unmodified PEI/DNA. We also use SAXS to monitor intermolecular assembly over time for zPEI and uPEI polyplexes.

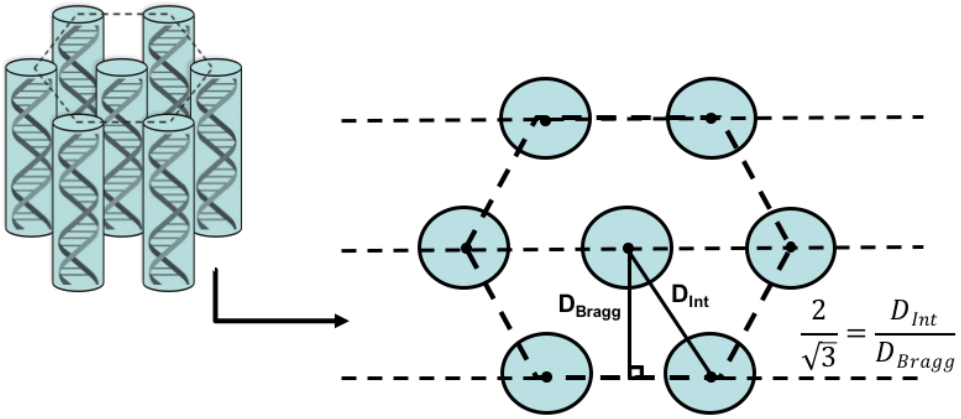

Figure 3.1. Polycationic complexes have been shown to pack into hexagonal lattice conformations.

3.2. Background on Small Angle X-ray Scattering

3.2.1. Generation of X-rays

Radiation with wavelengths between 0.1 and 100 angstroms are termed X-rays. Because these values are comparable in magnitude to the length of bonds and other interactions in condensed state materials, they are often used in diffraction experiments to characterize structure of said materials.[74-75] Kα radiation, with wavelength of 1.5418 angstroms is one of the most common wavelengths used in X-ray experiments, and is generated from electron bombardment of a copper target in an X-ray tube.[74-75] In this method of generation, commonly used for benchtop style X-ray scattering setups, a heated tungsten filament is used as a cathode, and a negative voltage is applied.[70] This results in the ejection of electrons, which are attracted to the anode due to a positive current applied, which is attached to the target metal.[74] Electrons striking the target metal result in X-ray production from two main mechanisms. The first is a broad range of wavelengths resulting

from the deceleration of electrons as they impact the target metal, termed bremsstrahlung ("brake radiation"). [74-75] Second, sharp peaks, or "characteristic radiation" is produced when impacting electrons result in ejection of core electrons from the metal target. [74-75] As higher energy electrons fall to fill this vacancy, photons with characteristic wavelengths (specific to type of metal used as target) are emitted depending upon which subshell electrons move from. [74-75] Because the impact of electrons generates heat, the amount of power applied to the tube and, consequentially the output of radiation, is limited. This can be partially overcome by using a rotating anode to limit heat buildup on the anode, or a liquid cooling system may be employed.[74] An alternative to X-ray tube setups capable of much higher radiation output, which allows for shorter periods of measurement and higher resolution, is use of a synchrotron source.[74] In this setup, electrons are radially accelerated on a circular track at speeds just below the speed of light.[74] The acceleration of the charged electrons produces a broad spectrum of high powered radiation.[74] In either synchrotron or tube based setups, output radiation must often be filtered to include only the wavelength range of interest to the experimenter. Often this is accomplished by nickel filtration, the use of crystal monochromators, or polycrystalline filters.[74]

3.2.2. Small Angle X-ray Scattering (SAXS) Theory

In order to discuss X-ray scattering experiments, terminology used must be carefully established. When X-ray radiation impacts a sample, the radiation is displaced in all directions by the electrons in the sample, termed scattering.[74] When X-rays are

scattered by a sample possessing order, such as a crystal or a polycrystalline material, the scattered rays interfere either constructively or destructively with each other, limiting which scattered angles can be detected.[74] This scattering and resulting interference in ordered samples is defined as diffraction.[74] It is common, however, to interchangeably use these terms, especially when discussing techniques such as small angle scattering (SAXS) or wide angle scattering (WAXS), both which make use of diffraction.[74] X-rays, like all electromagnetic radiation, possess both wave and particle behavior.[74] They propagate through space as waves with electronic and magnetic components, both with periodically repeating amplitudes (over the course of 1 wavelength).[70, 74, 78] In order for constructive interference to occur, parallel photons of light must have overlapping wave functions.[70, 74, 78] In X-ray scattering experiments, a wavelength of radiation is chosen that is on the same magnitude as the spacing of ordered structures in the samples.[74] Figure 3.2 portrays X-ray beams impacting a sample of ordered lattice structure with interplanar distance d_{Bragg}.[70] Radiation scatters off of the top most plane at an atom/molecule at point Z, and off of the second plane at point B.

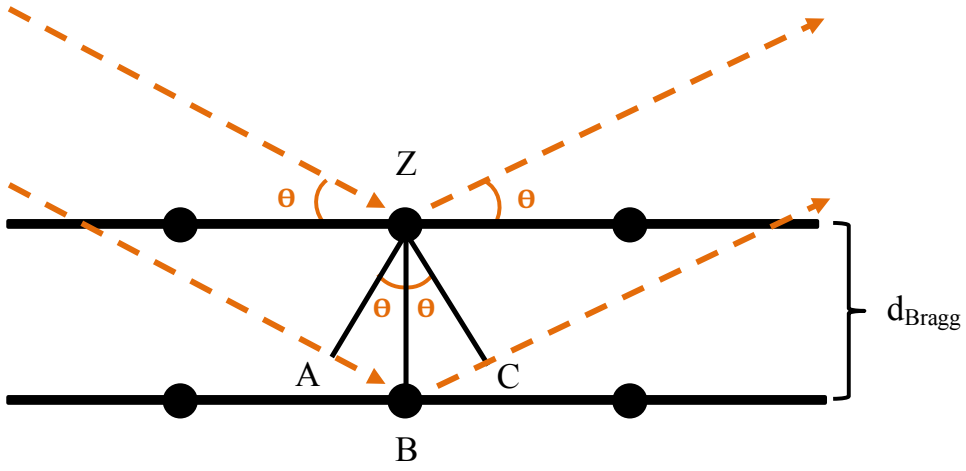

Figure 3.2. Representation of radiation scattering off of a crystalline packing pattern. Image based upon Figure 12-6 (pp. 279) in chapter 12 of Skoog, Holler, and Nieman's Principles of Instrumental Analysis (5th ed). Radiation depicted as orange dotted lines scatters off of molecules Z and B that lie in parallel crystal planes in a simple cubic packing pattern.

In order for the two wave functions to overlap and constructively interfere with one another, the additional distance travelled by the light scattered off of point B must be equal to some integer multiple of the wavelength.[70]

$$AB + BC = n\lambda \qquad \text{(Equation 3.1)}$$

Since AB and BC are equal to $d_{Bragg}\sin\theta$, the conditions for constructive interference can be summed up by the following equation[70]:

$$n\lambda = 2d_{Bragg}\sin\theta \qquad \text{(Equation 3.2)}$$

This is known as Bragg's law, and defines at what angles diffraction can occur. For crystalline samples made up of one orientation of ordered packing structure, this would result in defined points of diffraction on a flat imaging surface. When a sample is made up of many orientations of the same unit structure; such as powders, liquids, or the DNA

suspensions examined in this study, the projected diffraction image will be a ring of a radius proportional to the angle of scattering. If the distance between the detector and sample is known, the angle of scattering can be established, and d_{Bragg} can be calculated using Braggs law. Standards, such as silver behenate, with defined series of Bragg spacings, are commonly used to calibrate the sample to detector distance for SAXS.[79-80] If the unit cell type can be established, distance between molecules can be calculated from the d_{Bragg} value. For instance, in a hexagonal lattice unit cell, such as those observed in polycation/DNA complexes, the interhelical spacing (d_{int}) of DNA molecules represented in figure 3.1 above could be calculated as follows:

$$d_{int} = \frac{2}{\sqrt{3}} d_{Bragg} \qquad \text{(Equation 3.3)}$$

Scattering experiments are usually divided into 3 categories based on angles of diffraction measured: wide angle x-ray scattering (WAXS) is the measurement at angles greater than 10° (d_{Bragg} < 1 nm), small angle x-ray scattering (SAXS) the measurement of angles between 0.1 and 10° (100 nm > d_{Bragg} > 1 nm), and ultrasmall angle x-ray scattering (USAXS) the measurement of angles less than 0.1° (d_{Bragg} > 100 nm).[76] To measure smaller angles, the distance between the detector and the sample must be longer. Because the angle of scattering is inversely proportional to the spacing of the unit cell planes, the dimensions of image projected onto the detector are inversely proportional to the dimensions of the material being imaged. For this reason, it is often useful to describe the dimensions of the image in units of inverted distance, or inverse space. In our experiments, we use q (nm^{-1}) to describe the magnitude of radial scattering:

$$q = \frac{4\pi sin\theta}{\lambda} \qquad \text{(Equation 3.4)}$$

3.3. Materials and Methods

3.3.1. Materials

In addition to the synthesized zPEI described in chapter 2, the following materials were also used. 10 mM tris (400 μM NaN_3) was prepared from Tris HCl purchased from Madiatech, Inc (Manassas, VA) and sodium azide from Sigma Aldrich (St. Louis, MO). Calf-thymus DNA was purchased from Sigma Aldrich (St. Louis, MO) and suspended in 10 mM tris (400 μM NaN_3) as recommended by the manufacturer.

3.3.2. Sample Preparation

Concentrated PEI solution (0.5-1 mg/ml) was added to 300 μg of calf-thymus (CT) DNA suspended in 10 mM tris buffer (400 μM NaN_3) to the desired PEI/DNA weight ratio resulting in complete condensation of DNA. UV/Vis of the supernatant confirmed complete DNA condensation. Samples were made in triplicate. Samples were allowed to incubate at room temperature for 30 minutes, then centrifuged at 10500 g for 10 minutes. The condensate gives a white pellet. The condensate was then removed by a glass rod and placed in 1 mL of 10 mM tris (pH 7.5) buffer and allowed to equilibrate. Samples were measured after 1 hour, 1 day, 1 week, 3 weeks, and 1 month of incubation. For SAXS measurements, equilibrated pellets were placed in a home designed Teflon sample holder,

sealed between Mylar windows in fresh buffer, and measured as described in the instrumental setup section. For time series measurements, after x-ray exposure, samples were placed back into fresh 1 mL Tris buffer to equilibrate further until subsequent measurement. In order to determine sample to detector distance, silver behenate was mounted in the same sample holder and exposed to x-ray radiation.

3.3.3. Instrumental Setup

A Nonius FR-591 rotating-anode fine-focus X-ray generator (45 kV and 20 mA) was used to produce Cu$K\alpha$ radiation (1.54 Angstroms). Detection was imaged using a Bruker SMART-6000 Phosphor CCD detector. The teflon sample holder was placed in a steel holder (figure 3.3a) to mount the DNA pellet in the path of the source radiation. The pellet was placed in the top of the triangular open window on Teflon holder A, in buffer. This window was flanked by Mylar films to hold the sample within the holder. The sandwich assembly was then placed inside of the steel sample holder, with the triangular portion pointing down, so that the DNA pellet was aligned through the small circular hole in the holder. This was mounted between the radiation source and the detector with the x-ray beam aligned to allow passage through the sample. A helium chamber was placed between the sample and the detector to minimize scattering from air. At the back of the helium chamber, a lead beam stop was used to prevent the direct beam from reaching the detector. Samples were typically exposed for 2 minutes. A photo of this setup is displayed in figure 3.3b. Once imaged by the detector, Fit2D software was used to radially integrate

the circular diffraction patterns. Origin software was subsequently used to plot scattering profiles and determine Bragg peak positions. A representative SAXS diffraction pattern of PEI/CT-DNA polyplex is shown below, along with a radial integration displayed in units of intensity vs. inverse space (figure 3.4).

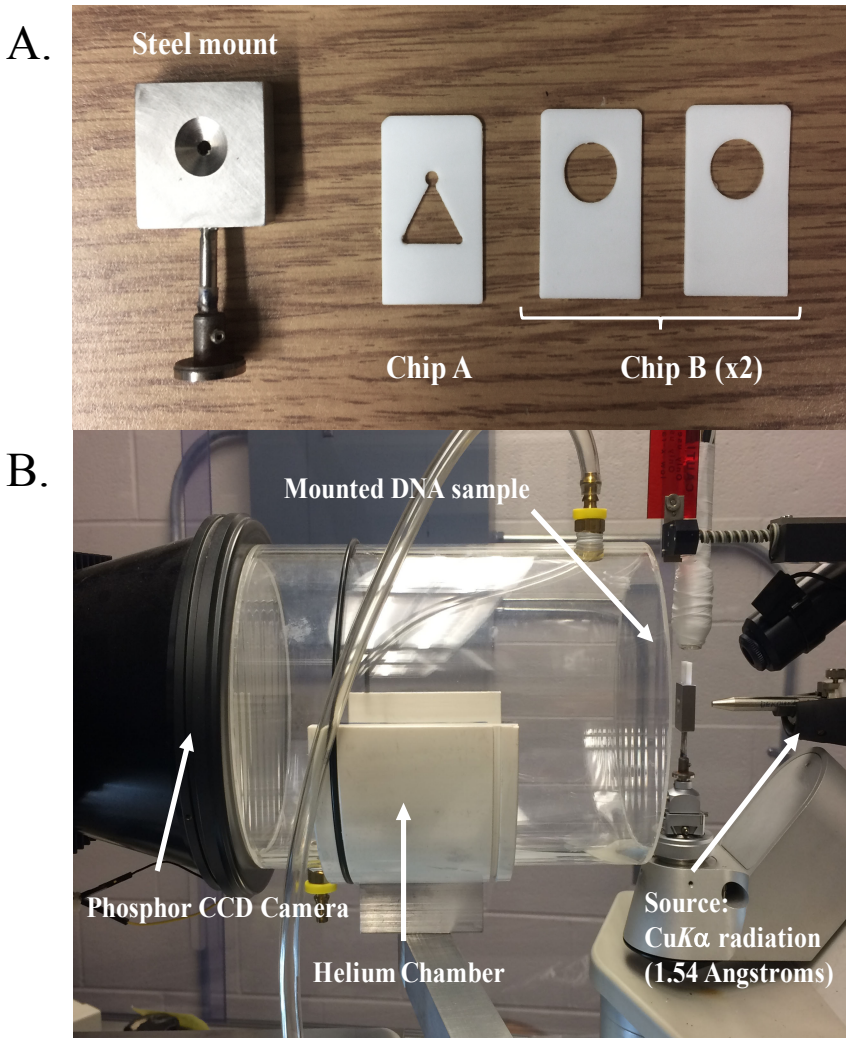

Figure 3.3. A. The teflon chips and steel mount used to hold the polyplex pellet in place. B. SAXS setup used to collect data.

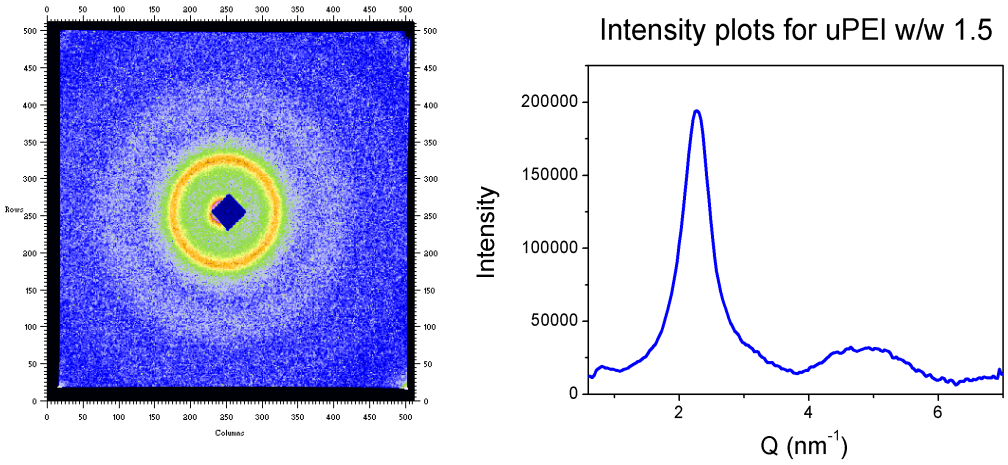

Figure 3.4. Left: Scattering diffraction pattern of a PEI/DNA polyplex complexed at a weight ratio of 1.5. A beam stop is visible as a dark diamond. Right: Radial integration from the center of the imaged scattering profile. A clear Bragg peak at a q value of ~2.3 nm^{-1} is visible.

3.4. Results and Discussion

In order to better understand the packing of PEI/DNA complexes as a function of percent succinylation, a series of SAXS samples were made and measured at various time points over a period of 1 month. In addition to the unmodified, 5.8 %, 8.0 %, 26.7 %, and 35.0 % zPEI were all measured after 2 hours, 25 hours, 1 week, and 1 month. Representative scattering profiles of each zPEI/DNA complex are shown below in figure 3.5. A collection of representative samples observed after 1 week of incubation is shown below in figure 3.6. Bragg spacings are observed to vary considerably with zwitterionic character. At lower percent substitutions (5.8 % and 8.0 %) the Bragg spacings are

increased above those measured for unmodified PEI. This is consistent with previous results by the DeRouchey lab using arginine peptides which showed the insertion of a negative moiety greatly increased the intermolecular repulsions resulting in significantly larger interaxial DNA spacings.[81] Surprisingly, at 26.7% and 35.0% succinylation, this trend is reversed, and DNA-DNA spacings decrease significantly below even unmodified PEI-DNA.

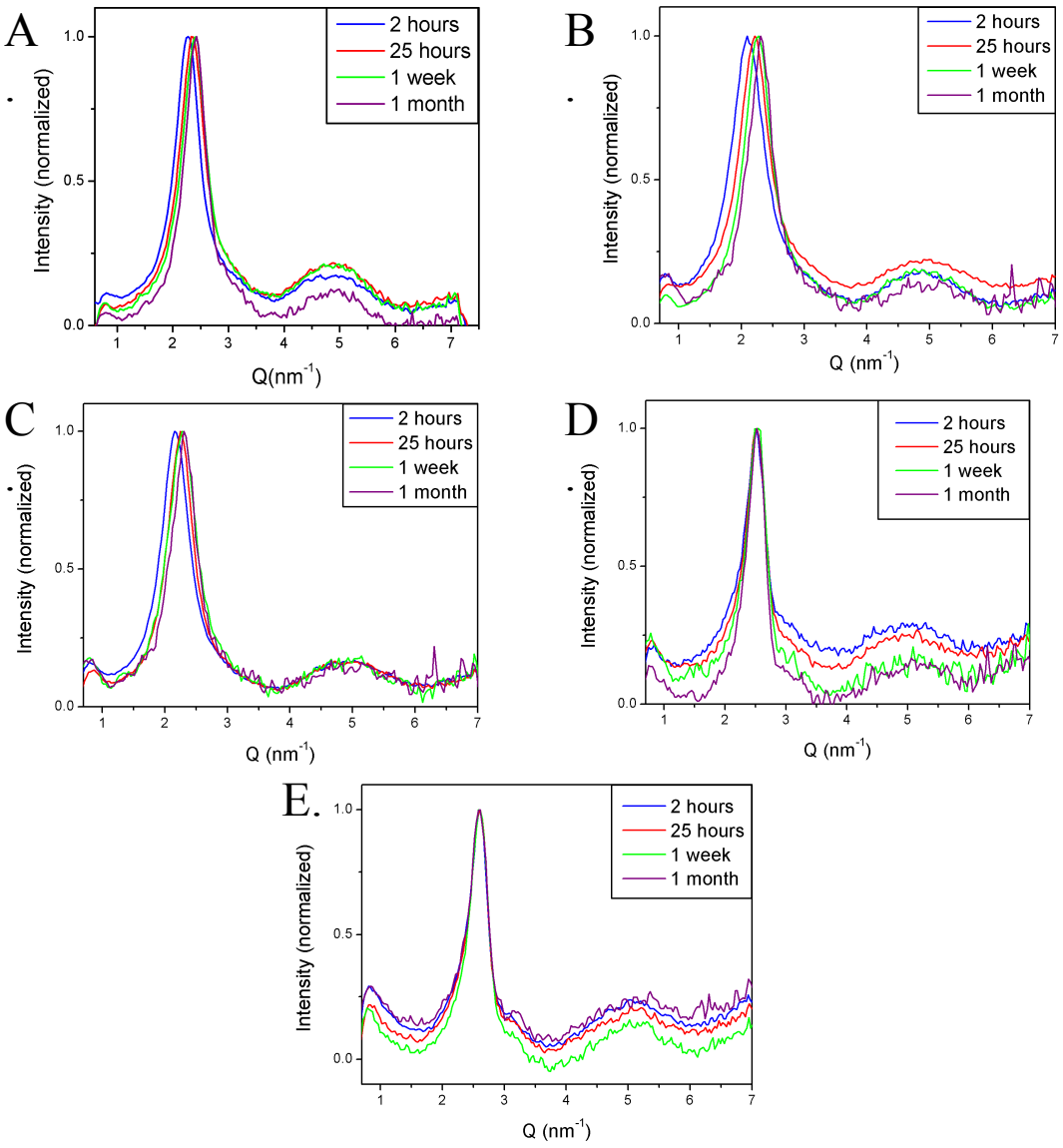

Figure 3.5. Plots of intensity vs. Q (nm^{-1}) for PEI derivatives complexed with CT-DNA a. unmodified PEI w/w 1.5 b. 5.8% zPEI w/w 2 c. 8.0% zPEI w/w 3.1 d. 26.7% zPEI w/w 4.1 e. 35.0% zPEI w/w 6.1. Weight ratios chosen that resulted in complete binding of DNA

A plot of Bragg spacings for each sample after 1 week is shown below in figure 3.7. While binding and release gels discussed in chapter two behaved as expected with increased zwitterionic character leading to reduced strength of DNA interaction, these x-

ray results are unexpected. Previous work in the DeRouchey lab on a similar system, a succinylated variant of the cationic dendrimer G4 polyamidoamine (zPAMAM), visualized a time and substitution % dependent phase transition. When unmodified G4 PAMAM and CT-DNA were mixed at "low salt" conditions, similarly to how zPEI samples were

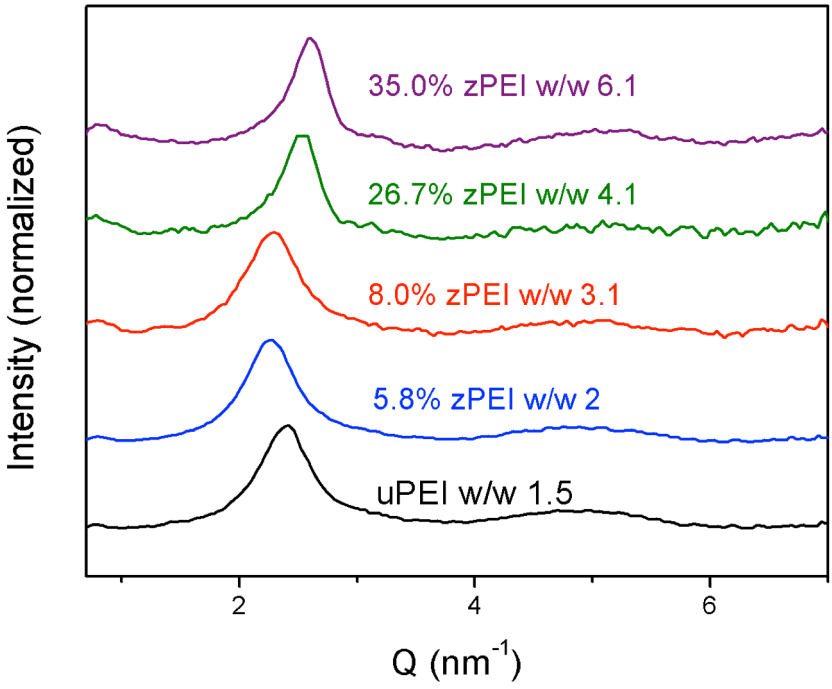

Figure 3.6. Plots of intensity vs. Q (nm^{-1}) for PEI derivatives complexed with CT-DNA following one week of incubation. Weight ratios chosen that resulted in complete binding of DNA.

prepared in this study, two distinct peaks were visible during the first two weeks of incubation.[81] These peaks were consistent with a columnar square lattice and a columnar hexagonal lattice. Over a few months, the square lattice peak disappeared and only the energetically favored hexagonal phase was observed. The use of a high salt preparation was observed to overcome this barrier resulting in only a hexagonal phase being observed.

Interestingly, the zPAMAM/DNA samples even prepared with the high salt preparation showed the same biphasic behavior as the low salt prepared PAMAM/DNA. With increasing percent modification, the dominant Bragg peaks observed in zPAMAM/DNA shifted from the hexagonal phase to the square lattice phase. One possible explanation for the changing trends in DNA-DNA spacings with zPEI percent modification could be a phase transition resulting in a smaller DNA-DNA spacing. Unfortunately, all of the SAXS spectrum taken on zPEI/DNA only contained one Bragg peak making it difficult to ascertain information related to the DNA lattice in zPEI. As the packaging in zPEI/DNA is unclear, for comparative purposes, all measurements reported in this chapter are given as the phase-independent Bragg spacings instead of the interhelical spacings calculated for a hexagonal lattice.

The square lattice phase observed in G4 zPAMAM occurs at a larger Bragg spacing than the hexagonal DNA lattice. Similarly, one would predict for a similar transition in zPEI, we would observe an increase in the Bragg reflection. However, for the higher percent modifications (26.7% and 35%) we see the opposite with DNA-DNA spacings being even smaller than unmodified PEI/DNA. G4 PAMAM contains 256 primary amine groups localized to the outside of the branched dendrimer. Since DNA likely shows preferential interaction with the outer primary amines as opposed to the uncharged tertiary amines on the inside of the dendrimer, the interactions and conformational shifts between the dendrimer and DNA are likely very different from those observed in a branched PEI molecule, which can interact with DNA through both primary and secondary amines located both on the outside and inside of the random branching structure.

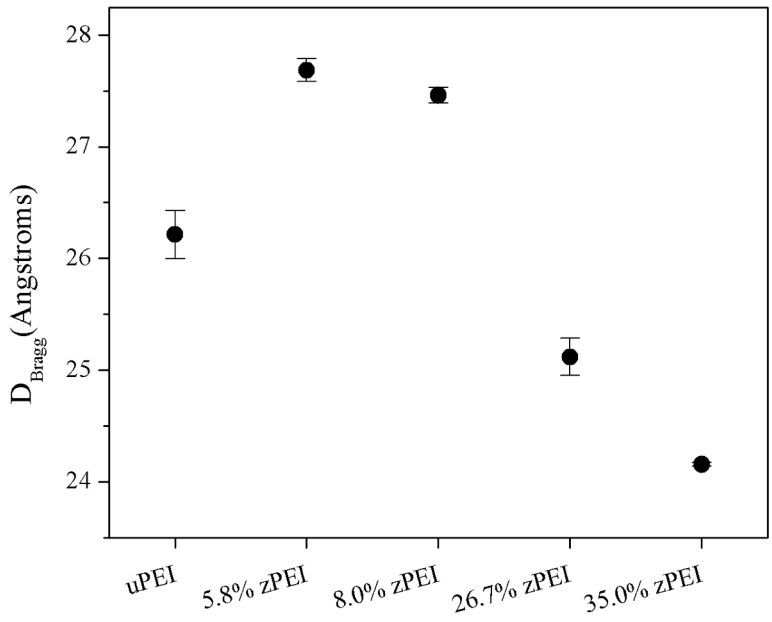

Figure 3.7. Bragg spacings of zPEI samples collected after 1 week incubation. Each sample complexed at a weight ratio that resulted in complete DNA binding.

Plots of d_{Bragg} vs time for all samples measured are shown in figure 3.8. Unmodified PEI, along with 5.8 % and 8.0 % zPEI, show a time dependent rearrangement of approximately 5% over one month to smaller DNA-DNA spacings. Samples of 26.7% and 35.0% zPEI, however, show significantly less rearrangement over time, reaching a stable conformation in under 24 hours. This suggests that the zwitterionic character of the zPEI is reducing kinetic energy barriers allowing for faster equilibrium structures to be achieved over significantly shorter time scales.

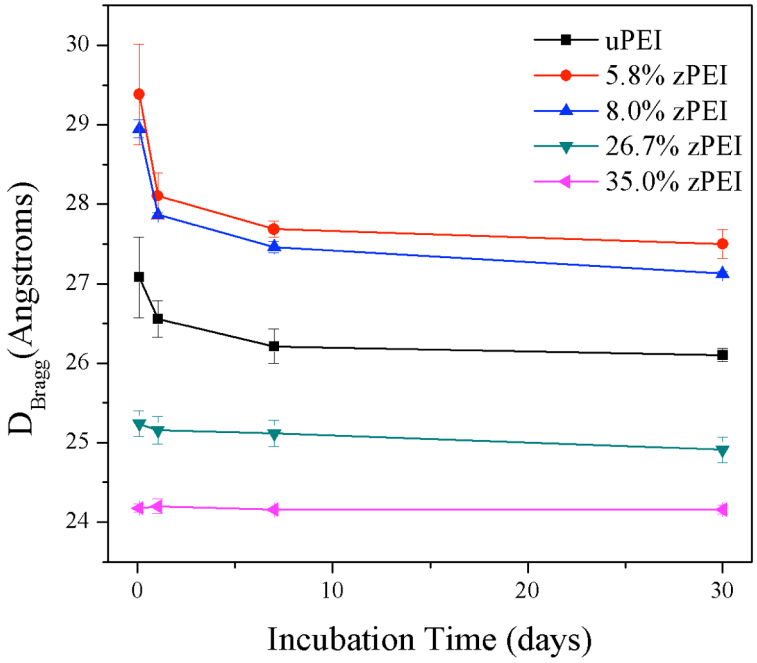

Figure 3.8. Bragg spacings of zPEI samples collected over the course of 1 month. Each sample complexed at a weight ratio that resulted in complete DNA binding.

3.5. Conclusions and Future Work

The internal structure of succinylated PEI/DNA polyplexes were investigated by SAXS analysis. At lower polymer substitution ratios, increased succinylation appeared to cause an increase in the Bragg spacing of complexes, which can be interpreted as an opening of polyplex structure due to loosened charge interactions. Unexpectedly, at higher substitution ratios, zPEI complexed DNA at lower Bragg spacings than observed with the

unmodified polymer. Additionally, the higher percent modified zPEI complexes showed significantly shorter time scales to achieve equilibrium structures. Taken together with the agarose gel studies (Ch. 2) which indicated loosened DNA/polymer interactions with increasing succinylation, these observations are surprising. One possible suggestion is that higher percent modifications in zPEI result in a phase transition to a smaller DNA-DNA spacing in the condensates. To better understand the kinetic barriers to polyplex structural rearrangement, and the effect of succinylation upon them, a "high salt" preparation, involving combining concentrated solutions of DNA and polymer in a 2 M solution of NaCl, may be performed on zPEI in the future. The high salt concentration prevents the DNA from condensing, allowing both solutions to be mixed homogeneously. Condensation is induced by the addition of buffer, decreasing the salt concentration until DNA/polymer condensation occurs. By allowing for homogenous mixing prior to condensation, this preparation was shown by DeRouchey et. al. to bypass the time consuming kinetic rearrangement of DNA/polycation complexes.[77] Future work should also focus on better methods to accurately identify the nature of the succinylation reaction in zPEI and possible phase transitions. Observation of possible higher order reflections to allow for assignment of DNA lattice would require a synchrotron source. Orienting DNA samples may also improve scattering profiles. With this type of instrumentation, it may be possible to differentiate different lines of symmetry within the structure, and properly determine lattice conformation as has been previously done by DeRouchey et al.[77]

Appendix Section: Diffusion in Polymer Gels with Competing Interaction Sites

A.1. Introduction

Biogels, made up of polymer networks diffusing in an aqueous environment, perform a variety of physiological functions in organisms, from the lubrication of joints to regulation of molecular diffusion.[82] Fluids containing networks of carbohydrates and proteins make up biogels such as the extracellular matrix, epithelial mucus, and the basal lamina of blood vessels are able to regulate passage of messenger molecules, nutrients, pathogens and other substances to cells.[82] Electrostatic interaction, in addition to steric filtration based upon size, has been determined to be one of the mechanisms utilized in filtration of biological fluids.[83-84] In fact, studies on extracellular matrix and mucin hydrogels reveals that charge particles may be filtered based upon the magnitude of charge, rather than the sign of the charge itself.[83, 85] Previous collaborative work between the laboratories of Dr. Jason DeRouchey (Chemistry department, University of Kentucky; Lexington, Ky) and Dr. Roland R. Netz (Physics department, Free University of Berlin; Berlin, Germany) have demonstrated the importance of attractive forces in limiting of diffusion of particles in charged hydrogels.[86]

Because real biological fluids are heterogeneous mixtures of biopolymers with disparate chemical and physical properties; models that better approximate real biogels, containing both attractive and repulsive forces, must be constructed and experimentally validated. To measure the diffusion of nanoparticles in solutions, such as polymer systems and tissues, fluorescence correlation spectroscopy (FCS) has previously been utilized. [86-91] FCS allows for measurement of diffusion coefficients (D, $\mu m^2/s$) of probe molecules

through time autocorrelation of detected fluorescent intensity fluctuations in a diffraction limited confocal volume. FCS only measures diffusion of particles that fluoresce at wavelengths chosen, making the technique highly selective. Additionally, the diffraction limited spot in solution measured can be on the order of fL, and the concentration of particles needed for accurate measurement ranges from pM-nM. This allows for reduced material consumption in sample preparation as well as limited particle interactions in solution.

Mixed charge gel solutions comprised of positive and negative dextran polymers were created and the diffusion of a negatively charged probe molecule (Alexa 488) was experimentally measured with FCS. Experiments were subsequently compared to simulated models of mixed charged gels developed by the Netz lab. Their model approximates a mixed charge gel as sets of fibers with random distributions of charged "patches" of either positive or negative charge, and finds that particle trapping, and thus retardation of diffusion, occurs in locations of the gel containing high densities of charge opposite to that of the diffusing particle.[92] Our experimental results were found to be in quantitative agreement with the model.

A.2. Materials and Methods

A.2.1. Materials

The following Dextrans were purchased through Sigma Aldrich: Dextran (M_w = 500 kDa), Dextran (M_w = 15-25kDa), diethylaminoethyl-dextran (DEAE-dextran(+),M_w = 500kDa) and Carboxymethyl-dextran (CM-dextran(-),M_w = 15-20kDa). The 500 kDa and 15-25 kDa dextrans are neutrally charged, while DEAE dextran possesses positively charged diethylaminoethyl groups, and CM dextran negatively charged carboxymethyl groups. The following fluorescent dye molecules were purchased from Fisher Scientific: Alexa Fluor® 488 Succinimidyl Ester dye (Alexa488, Abs/Em peak: 495/519 nm), and Rhodamine 110 (R110, Abs/Em peaks: 496/520 nm). The fluorescent molecules were readily soluble in water, and did not require purification prior to use.

A.2.2. Preparation of Dextran Solutions

Dextran stock solutions were prepared by dissolving solid dextran in 10 mM MES buffer (pH = 6.4) to a final concentration of 8-20 % w/v. Solutions were allowed to mix for 24 hours following preparation to ensure homogeneity. Stock solutions were used to prepare experimental samples of appropriate concentration by dilution into buffer to a final volume of ~500 μL. These solutions were mixed and allowed to equilibrate for an additional 24 hours. For mixed solutions of DEAE and CM dextran, stock solutions of each were added together to achieve the desired volumetric ratio of each dextran with

respect to total dextran. Alexa 488 dye was added to a total concentration of ~5-10 nM, and this final solution was allowed to incubate, protected from light, for at least 6 hours before measurement to allow adequate dispersal of the dye molecule throughout solution. Samples were loaded into NUNC LabTek 8-well microscopy chambers (Nalge Nunc, Penfield, NY) prior measurement by FCS.

A.2.3. FCS Setup

An Alba fluorescent fluctuation system (FFS) confocal system was used for all fluorescence correlation spectroscopy (FCS) experiments. A continuous wave 488 nm laser diode was used as an excitation source. Excitation light was directed into experimental samples through a Nikon Ti-U microscope (60x/1.2 NA water-immersion objective lens). Emitted light was passed through a 514-nm long-pass filter and a 50/50 beam splitter into two pinhole equipped Hamamatsu H7422P-40 photomultiplier tubes for detection. Confocal volume dimensions (w_0 and z_0) were determined through measurement of aqueous Rhodamine 110 at known concentrations ($D = 440\ \mu m^2\ s^{-1}$).[93] Routine realignments of detector pinhole/lens sets were performed with R110. In order to test solution homogeneity, reported results are the average of at least 9 measurements in different locations in solutions. Sampling times of 30 seconds were used for all measurements. A sampling frequency of 200,000 Hz was used, which allowed autocorrelation over $\tau > 5.0\ \mu s$. All fitting was executed through VistaVision 4.0 software (VWR, Radnor PA).

A.2.4. FCS Data Analysis

Many have already reported on the theory behind fluorescence correlation spectroscopy, so a brief synopsis will be described here. [94-95] The measured time traces of fluorescent events at all times (t) are compared for self-similarity after a lag time (τ) by calculation of the normalized cross correlation, G(τ):

$$G(\tau) = \frac{<\delta F(t)_R \delta F(t+\tau)_L>}{<F(t)_R><F(t)_L>} \qquad \text{(Equation A.1)}$$

$\delta F(t)$ and $\delta F(t+\tau)$ represent deviation from the mean fluorescence $< F(t) >$ at time t and after time t + τ. Cross correlation between two different detectors ensures that the resulting autocorrelation is free from the effects of detector after-pulsing. [95] Assuming that all fluctuations are due to uniform fluorescent particles diffusing in and out of the confocal volume by Brownian motion, the following autocorrelation fit was used to model diffusive behavior:

$$G(\tau) = \frac{1}{N} \cdot \left(\frac{1}{1+\frac{\tau}{\tau_D}} \right) \cdot \frac{1}{\sqrt{1+\frac{w_0^2}{z_0^2}\cdot\frac{\tau}{\tau_D}}} \qquad \text{(Equation A.2)}$$

Where τ_D represents the dwell time of the particles in the confocal volume, whose shape can be approximated as a Gaussian ellipsoid with axial height z_0 and equatorial width w_0. N is the average number of particles occupying the observation volume. The translational diffusion coefficient D ($\mu m^2 s^{-1}$) can be calculated from τ_D and the equatorial width using

$$\tau_D = \frac{w_0^2}{4D} \qquad \text{(Equation A.3)}$$

In the case of spherical particles, the Stokes-Einstein equation can be used to relate the diffusion coefficient to the hydrodynamic radius (r_H), solution viscosity (η), and temperature (T):

$$D = \frac{k_B \mathrm{T}}{6\pi\eta r_h} \qquad \text{(Equation A.4)}$$

Here, k_B represents the Boltzmann constant. To facilitate visual representation and understanding, autocorrelations and fits can be normalized by dividing by G(0) and graphed with τ_D on a logarithmic scale.

A.3. Results and Discussion

Fluorescence correlation spectroscopy (FCS) was used to measure diffusive properties of charged nanoparticles in solutions containing mixes of both positive and negatively charged polymers. Alexa 488 was selected as a suitable probe molecule due to the -2 charge it possesses at a neutral pH. Charged polymer solutions were made from DEAE Dextran (MW ~500 kDa, 1 DEAE (+) group per ~2 glucose monomers) and CM Dextran (MW ~13 kDa, 1 CM (-) group per ~4 glucose monomers). To account for steric effects, Alexa transport in neutral Dextran was also measured. Due to the differences in molecular weight between the DEAE and CM Dextrans, neutral dextran of comparable masses (500 kDa and 20 kDa, respectively) was examined. For simplicity, the charged polymers will be noted as dextran(+) and dextran(-), and the neutral polymers as dextran500 and dextran20. To ensure solution homogeneity, reported diffusion values for Alexa 488 are the average of 9 measurements in various solution locations. All solutions

were prepared from solid dextran stocks without further purification other than that of the manufacturer.

Normalized autocorrelations for pure solutions of dextran(+) and dextran(-) at different wt % ratios are shown in figure A.1. Previous studies in the DeRouchey examined Alexa Fluor transport in Dextran(+) and dextran (-) solutions up to 8 wt%. Here, we also examined higher wt% solutions up to 15wt%. As was previously observed by the DeRouchey lab, transport in DEAE dextran was slowest in low wt% solutions (e.g. 2 wt%) but the measured dwell times by FCS got shorter at higher wt%. This trend continued at the high wt% solutions studied in this work. The shift to faster diffusion at higher concentrations of DEAE dextran is likely due to higher concentrations of counter-ions carried along with the positive dextran, which would screen some of the charge interaction between the negative dye and the positive DEAE groups.[86] Transport through pure dextran(-) solutions showed the opposite trend, in that as concentration of CM-dextran was increased, so too did the speed of diffusion. Translational diffusion coefficients for Alexa 488 in various unchared Dextran concentrations (% weight volume) is plotted in figure A.2. Low wt % results are in very good agreement with the previous report. Previously, the dextran stock had been dialyzed against ddH_2O in order to ensure purity of materials and remove excess salt.[86] As our diffusion values for non-dialyzed samples were nearly identical to dialysized dextrans, we showed that excess salt content or other contamination is very low and can readily be discounted as a source of experimental deviation. For the next studies, we therefore used Dextran solutions as received without dialysis and lyophilization. In dextran(+) solutions, diffusion of negative Alexa 488 is greatly reduced compared to the similarly massed dextran500, likely due to electrostatic interaction

between opposite charges. Probe diffusion is roughly comparable between dextran(-) solutions and the neutral dextran20, suggesting attractive, rather than repulsive,

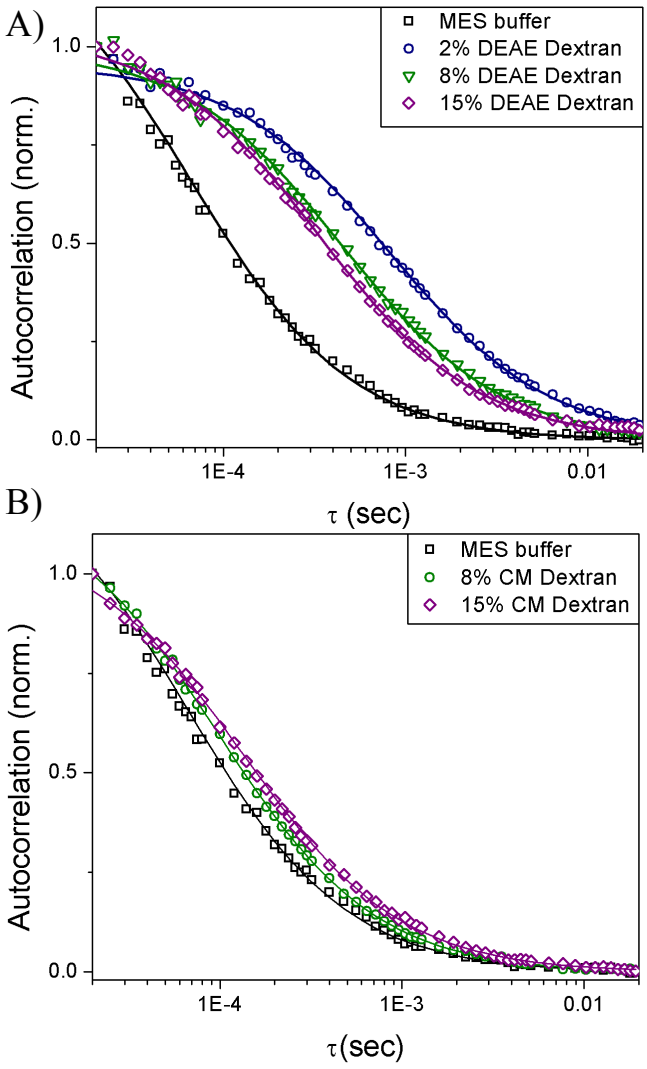

Figure A.1. Characteristic normalized FCS autocorrelation curves of diffusion of Alexa 488 NHS ester (-2 charge) through a 10 mM MES buffer (pH = 6.4) solution of (A) select wt% dextran (+) and (B) select wt% dextran (-). Experimental autocorrelations (symbols) are fit (solid lines) as previously described in order to acquire translational diffusion coefficients.

electrostatic forces play a large role in modulation of nanoparticle diffusion through a polymer solution.

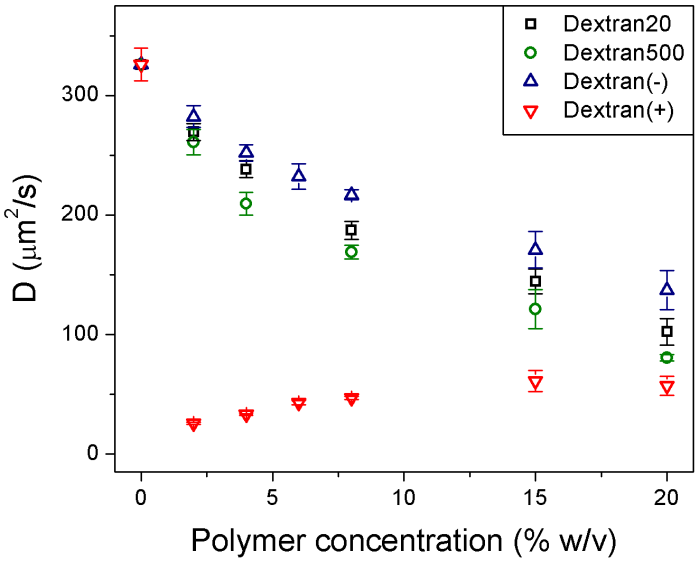

Figure A.2. Translational diffusion coefficients (D) of Alexa 488 in increasing concentrations (% wv) dextrans. All values acquired through fits of experimental FCS autocorrelations.

Mixed charge dextran solutions were prepared by addition of varying volumes of equal wt % solutions of dextran(+) and dextran(-) together, followed by mixing and incubation at room temperature overnight. Charge mixing ratios are represented as volume of dextran(-)/total dextran volume. For concentrations below 4% weight per volume (wv), mixing ratios of 0.75-0.9 volume dextran(-)/total dextran resulted in cloudy solutions that were inhomogeneous and unsuitable for FCS studies. One possible reason for this is that at concentrations below 4% wv, the concentration of salt from the commercial Dextran stock are low enough in solution that the release of counter-ions into solution becomes an entropically favorable condition for complexation between the positive and negative

dextran to form a coagulate. Representative FCS autocorrelation curves of Alexa 488 diffusion through varying volumetric ratios of the positive dextran to the negative dextran at a total dextran concentration of 6% wv are shown in figure A.3. Larger amounts of dextran(-) with respect to dextran(+) are necessary to shift the dwell times of the probe molecule. This is at least partially explainable by the smaller number of monomers per charged group on dextran (+) compared to dextran (-). However, the previous report on probe diffusion through charged dextran showed that repulsive charge between dye and dextran resulted in a small increase in τ_D compared to neutral dextran, where an attractive force produced a significant increase in dwell time.[86] It is therefore reasonable to assume that the observed imbalance between τ_D and ratio of dextran(-) to dextran(+) are a result of both factors. Translational diffusion coefficients for Alexa488 probe molecule in 4, 6, and 8% wv mixed dextran solutions are shown in figure A.4 for various mixing ratios of Dextran(+) and dextran (-). When dextran(+) and dextran(-) are mixed at a 1 to 1 ratio, diffusion coefficients are approximately the same as pure dextran(+). Mixing ratios of at least 0.75 dextran(-)/total dextran are necessary to observe a shift in the translational diffusion coefficient away from that of the pure dextran(+) solutions of the same total dextran concentration, suggesting that the presence of positive charge largely determines the diffusive behavior of the negative nanoparticle through the polymer solution. However, because translational diffusion values rise with increasing volume ratio of dextran(-)/total dextran, addition of negative charge does appear to screen the interaction between dextran (+) and the negative dye molecule.

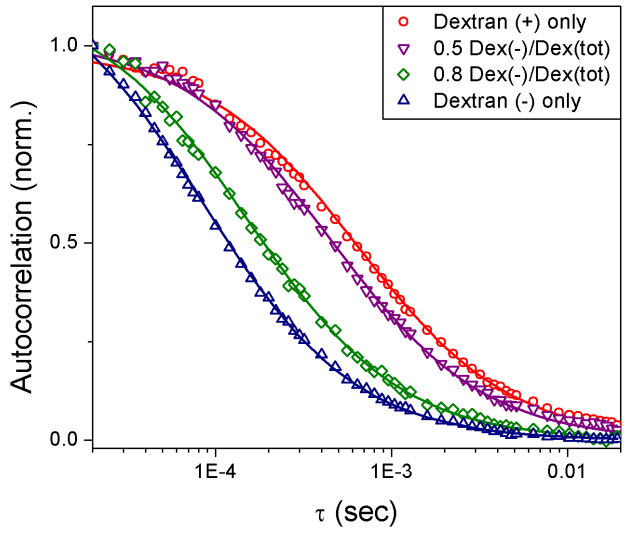

Figure A.3. Characteristic normalized FCS autocorrelation curves of diffusion of Alexa 488 NHS ester (-2 charge) through a 10 mM MES buffer (pH = 6.4) solution of 6% wt dextran at a variety of mixing ratios of equal concentrations of dextran(+) and dextran(-). Mixing ratios expressed as volume of dextran(-)/ volume total dextran. Experimental autocorrelations (symbols) are fit (solid lines) as previously described to acquire translational diffusion coefficients.

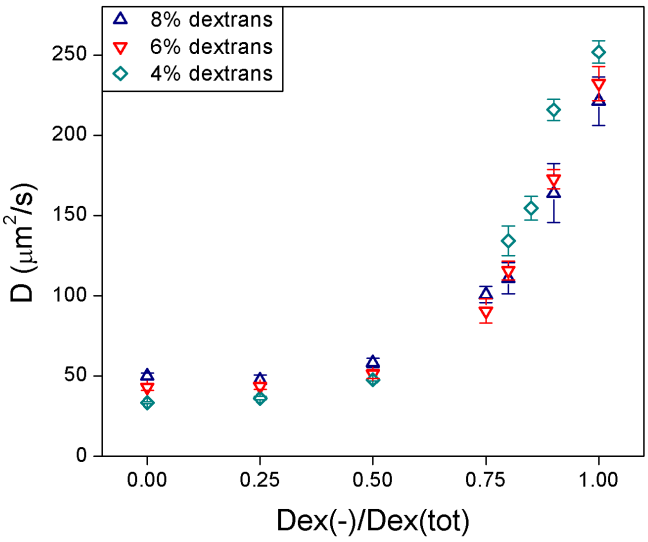

Figure A.4. Translational diffusion coefficients (D) of Alexa 488 in 4, 6, and 8 % wv mixed solutions of dextran(-) and dextran(+). D values are plotted against mixing ratio, expressed as volume of dextran(-)/ volume total dextran. All values acquired through fits of experimental FCS autocorrelations.

The Brownian dynamics (BD) simulation proposed by the Netz lab consist of a series of parallel rods, 16 oriented along the x, y and z axis for a total of 48 rods per three dimensional network.[92] Parameters are included for the Brownian motion of the particle, involving the internal energy and temperature, along with the distance between fibers (mesh size), diameter of the probe molecule. Disorder could be introduced into the square lattice structure of this network by increasing a term controlling the standard deviation of rod placement. Sections of the rods, designated "patches" were randomly assigned to be positively charged or negatively charged. A representative image of a disordered lattice of mixed charge is shown below in figure A.5. Notably, the probe particles were shown to

slow with increasing polymer concentration in networks with equal concentrations of positive and negative charge in both disordered and ordered systems in support of this idea suggested from the results of Lieleg and others.[83, 85]

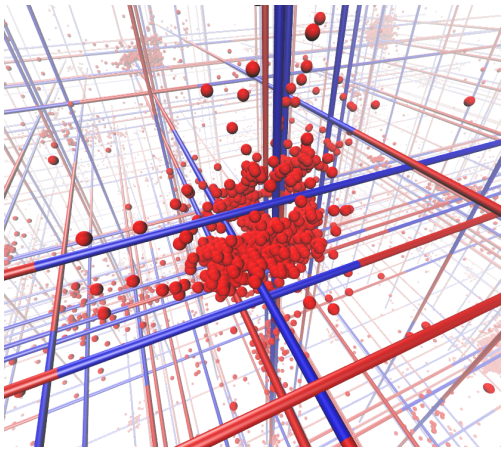

Figure A.5. Snapshot of a disordered lattice BD simulation. In locations of high negative charge (blue), the positive tracer is shown to localize, and become ensnared. Reprinted with permission from Hansing, J.; Duke, J.R.; Fryman, E.B.; DeRouchey, J.E.; Netz, R.R. Diffusion in polymer gels with competing interaction sites, 2017. Manuscript to be submitted for publication.

In order to experimentally validate the BD simulation proposed, the model was tuned to match the parameters of the mixed charged dextrans measured by FCS. By approximating the mesh size along with the charge per molecule, and the size and charge of Rhodamine 110, diffusion values for the mixing ratios and concentrations presented in figure A.4. were calculated. These values plotted against the experimentally determined diffusion coefficients, are plotted below in figure A.6. Calculated values are in quantitative agreement with measured values, except for in the 8% wv dextran solutions, where

simulated values appear to overestimate the diffusion of particles, likely due to a mis-estimation in the effect of hydrodynamic hindrance.

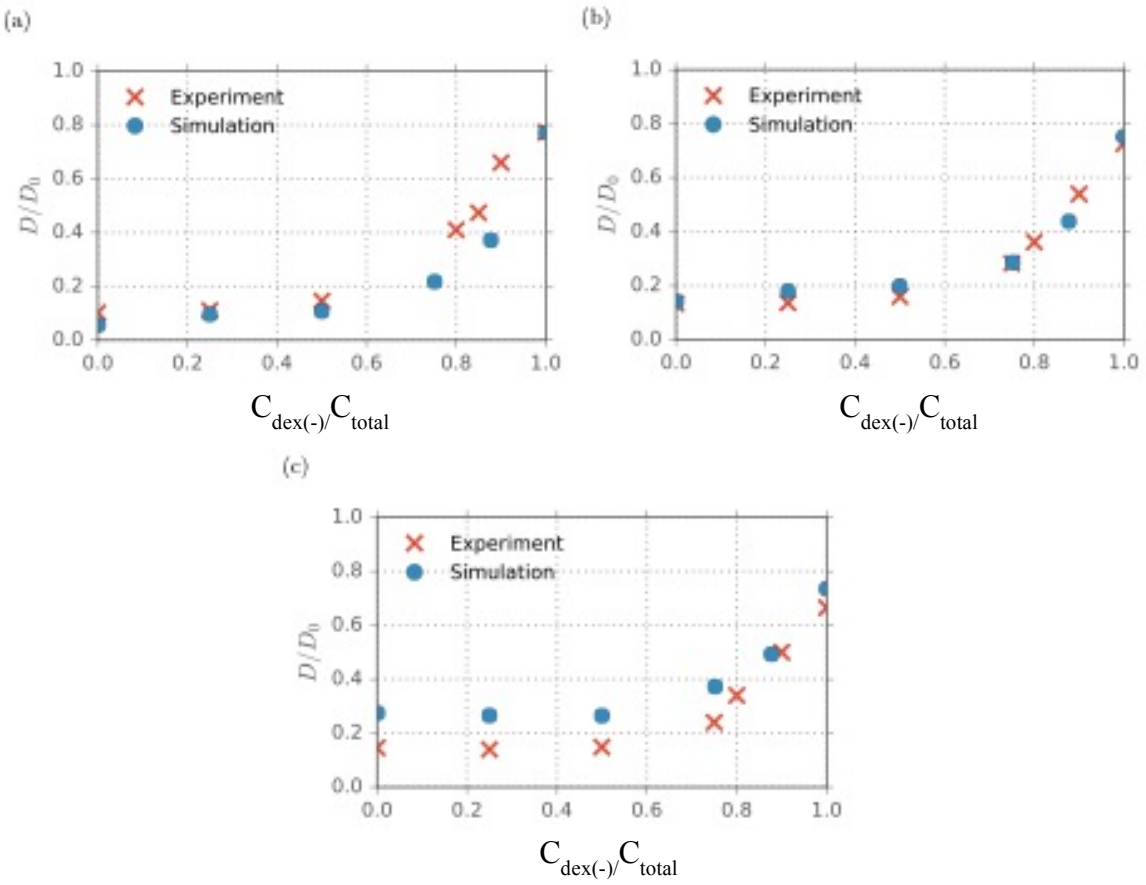

Figure A.6. Translational diffusion coefficients (D) of Alexa 488 in 4, 6, and 8 % wv mixed solutions of dextran(-) and dextran(+) presented against simulation data. D values are plotted against mixing ratio, expressed as volume of dextran(-)/ volume total dextran. Simulation data takes into account the ratio of 5/2 positive to negative charge between dextran(+) and dextran(-). Reprinted with permission from Hansing, J.; Duke, J.R.; Fryman, E.B.; DeRouchey, J.E.; Netz, R.R. Diffusion in polymer gels with competing interaction sites, 2017. Manuscript to be submitted for publication.

A.4. Conclusions

Using FCS, the diffusion of a negatively charged probe molecule in mixed and pure charged dextran solutions was measured. At mixing ratios between 0 and 0.75 negative to positive dextran, the diffusion of the negative probe molecule was nearly identical to diffusion in a purely positive dextran solution. This is in accordance with the idea that biogels possessing zwitterionic charge are able to filter out particles based upon the magnitude of charge, not simply the sign, proposed by Leileg and others. [83, 85] Brownian dynamic simulations by Hansing and Netz were found to also support this idea of filtration based upon magnitude, and a mechanism of particle entrapment in areas of high attractive charge density was observed in model networks. These simulations were found to be experimentally validated by the diffusion measurements carried out in mixed charge dextran solutions presented in this work. Future work may focus on creation of new zwitterionic polymer molecules to further validate simulations. Mixtures of CM and DEAE dextran are limited in that the charge density on each has not been tuned further than that of the manufacturer. Additionally, it would be interesting to see if the model system still finds agreement in polymer systems where patches of positive and negative charge occur on the same polymer molecule, rather than on separate chains. In this way, the level of disorder of charge may be modulated in gel solutions.

REFERENCES

1. Croce, C. M., Oncogenes and Cancer. *New England Journal of Medicine* **2008,** *358* (5), 502-511.
2. Ong, T.; Ramsey, B. W., Update in Cystic Fibrosis 2014. *American Journal of Respiratory and Critical Care Medicine* **2015,** *192* (6), 669-675.
3. Ramamoorth, M.; Narvekar, A., Non Viral Vectors in Gene Therapy- An Overview. *Journal of Clinical and Diagnostic Research : JCDR* **2015,** *9* (1), GE01-GE06.
4. Behr, J. P., GENE-TRANSFER WITH SYNTHETIC CATIONIC AMPHIPHILES - PROSPECTS FOR GENE-THERAPY. In *Bioconjugate Chem.*, **1994**; Vol. 5, pp 382-389.
5. Pack, D. W.; Hoffman, A. S.; Pun, S.; Stayton, P. S., Design and development of polymers for gene delivery. *Nat Rev Drug Discov* **2005,** *4* (7), 581-593.
6. Ginn, S. L.; Alexander, I. E.; Edelstein, M. L.; Abedi, M. R.; Wixon, J., Gene therapy clinical trials worldwide to 2012 – an update. *The Journal of Gene Medicine* **2013,** *15* (2), 65-77.
7. Grigsby, C. L.; Leong, K. W., Balancing protection and release of DNA: tools to address a bottleneck of non-viral gene delivery. *Journal of The Royal Society Interface* **2009,** *7* (Suppl 1), S67.
8. During, M. J., Adeno-associated virus as a gene delivery system. *Advanced Drug Delivery Reviews* **1997,** *27* (1), 83-94.
9. Vile, R. G.; Tuszynski, A.; Castleden, S., Retroviral vectors. From laboratory tools to molecular medicine. *Molecular biotechnology* **1996,** *5* (2), 139.
10. Anonymous, Calculated risks. *Nature* **2016,** *534* (7609), 590.
11. Dalby, B.; Cates, S.; Harris, A.; Ohki, E. C.; Tilkins, M. L.; Price, P. J.; Ciccarone, V. C., Advanced transfection with Lipofectamine 2000 reagent: primary neurons, siRNA, and high-throughput applications. *Methods* **2004,** *33* (2), 95-103.
12. Hönig, D.; Derouchey, J.; Jungmann, R.; Koch, C.; Plank, C.; Rädler, J. O., Biophysical characterization of copolymer-protected gene vectors. *Biomacromolecules* **2010,** *11* (7), 1802.
13. Finsinger, D.; Remy, J. S.; Erbacher, P.; Koch, C.; Plank, C., Protective copolymers for nonviral gene vectors: synthesis, vector characterization and application in gene delivery. *Gene Therapy* **2000,** *7* (14), 1183.
14. Scherer, F.; Schillinger, U.; Putz, U.; Stemberger, A.; Plank, C., Nonviral vector loaded collagen sponges for sustained gene delivery in vitro and in vivo. *The Journal of Gene Medicine* **2002,** *4* (6), 634-643.
15. Schillinger, U.; Wexel, G.; Hacker, C.; Kullmer, M.; Koch, C.; Gerg, M.; Vogt, S.; Ueblacker, P.; Tischer, T.; Hensler, D.; Wilisch, J.; Aigner, J.; Walch, A.; Stemberger, A.; Plank, C., A Fibrin Glue Composition as Carrier for Nucleic Acid Vectors. *Pharmaceutical Research* **2008,** *25* (12), 2946-2962.
16. Fant, K.; Esbjörner, E. K.; Jenkins, A.; Grossel, M. C.; Lincoln, P.; Nordén, B., Effects of PEGylation and acetylation of PAMAM dendrimers on DNA binding, cytotoxicity and in vitro transfection efficiency. *Molecular pharmaceutics* **2010,** *7* (5), 1734.

17. Ogris, M.; Brunner, S.; Schüller, S.; Kircheis, R.; Wagner, E., PEGylated DNA/transferrin–PEI complexes: reduced interaction with blood components, extended circulation in blood and potential for systemic gene delivery. *Gene Therapy* **1999,** *6* (4), 595.
18. Azzam, T.; Eliyahu, H.; Makovitzki, A.; Domb, A. J., Dextran-spermine conjugate: an efficient vector for gene delivery. *Macromolecular Symposia* **2003,** *195* (1), 247-262.
19. Eliyahu, H.; Makovitzki, A.; Azzam, T.; Zlotkin, A.; Joseph, A.; Gazit, D.; Barenholz, Y.; Domb, A. J., Novel dextran-spermine conjugates as transfecting agents: comparing water-soluble and micellar polymers. *Gene Therapy* **2005,** *12* (6), 494-503.
20. Zintchenko, A.; Philipp, A.; Dehshahri, A.; Wagner, E., Simple Modifications of Branched PEI Lead to Highly Efficient siRNA Carriers with Low Toxicity. *Bioconjugate Chemistry* **2008,** *19* (7), 1448-1455.
21. Forrest, M.; Meister, G.; Koerber, J.; Pack, D., Partial Acetylation of Polyethylenimine Enhances In Vitro Gene Delivery. *Pharmaceutical Research* **2004,** *21* (2), 365-371.
22. Gabrielson, N. P.; Pack, D. W., Acetylation of Polyethylenimine Enhances Gene Delivery via Weakened Polymer/DNA Interactions. *Biomacromolecules* **2006,** *7* (8), 2427-2435.
23. Sun, J.; Zeng, F.; Jian, H.; Wu, S., Grafting zwitterionic polymer chains onto PEI as a convenient strategy to enhance gene delivery performance. *Polymer Chemistry* **2013,** *4* (24), 5810-5818.
24. Sun, J.; Zeng, F.; Jian, H.; Wu, S., Conjugation with Betaine: A Facile and Effective Approach to Significant Improvement of Gene Delivery Properties of PEI. *Biomacromolecules* **2013,** *14* (3), 728-736.
25. Liu, X.; Yang, J. W.; Lynn, D. M., Addition of "Charge-Shifting" Side Chains to Linear Poly(ethyleneimine) Enhances Cell Transfection Efficiency. *Biomacromolecules* **2008,** *9* (7), 2063-2071.
26. Zauner, W.; Ogris, M.; Wagner, E., Polylysine-based transfection systems utilizing receptor-mediated delivery. *Advanced Drug Delivery Reviews* **1998,** *30* (1), 97-113.
27. Lungwitz, U.; Breunig, M.; Blunk, T.; Göpferich, A., Polyethylenimine-based non-viral gene delivery systems. *European Journal of Pharmaceutics and Biopharmaceutics* **2005,** *60* (2), 247-266.
28. Von Harpe, A.; Petersen, H.; Li, Y.; Kissel, T., Characterization of commercially available and synthesized polyethylenimines for gene delivery. *Journal of Controlled Release* **2000,** *69* (2), 309-322.
29. Suh, J.; Paik, H. J.; Hwang, B. K., Ionization of Poly(ethylenimine) and Poly(allylamine) at Various pH′s. *Bioorganic Chemistry* **1994,** *22* (3), 318-327.
30. Nagaya, J.; Homma, M.; Tanioka, A.; Minakata, A., Relationship between protonation and ion condensation for branched poly(ethylenimine). *Biophysical Chemistry* **1996,** *60* (1), 45-51.
31. Esfand, R.; Tomalia, D. A., Poly(amidoamine) (PAMAM) dendrimers: from biomimicry to drug delivery and biomedical applications. *Drug Discovery Today* **2001,** *6* (8), 427-436.

32. Tomalia, D. A.; Baker, H.; Dewald, J.; Hall, M.; Kallos, G.; Martin, S.; Roeck, J.; Ryder, J.; Smith, P., Dendritic macromolecules: synthesis of starburst dendrimers. *Macromolecules* **1986,** *19* (9), 2466-2468.
33. Leisner, D.; Imae, T., Polyelectrolyte Behavior of an Interpolyelectrolyte Complex Formed in Aqueous Solution of a Charged Dendrimer and Sodium Poly(l-glutamate). *The Journal of Physical Chemistry B* **2003,** *107* (47), 13158-13167.
34. Jin, G.-w.; Koo, H.; Nam, K.; Kim, H.; Lee, S.; Park, J.-S.; Lee, Y., PAMAM dendrimer with a 1,2-diaminoethane surface facilitates endosomal escape for enhanced pDNA delivery. *Polymer* **2011,** *52* (2), 339-346.
35. Lukacs, G. L.; Haggie, P.; Seksek, O.; Lechardeur, D.; Freedman, N.; Verkman, A. S., Size-dependent DNA Mobility in Cytoplasm and Nucleus. *Journal of Biological Chemistry* **2000,** *275* (3), 1625-1629.
36. Abdelhady, H. G.; Allen, S.; Davies, M. C.; Roberts, C. J.; Tendler, S. J. B.; Williams, P. M., Direct real-time molecular scale visualisation of the degradation of condensed DNA complexes exposed to DNase I. *Nucleic Acids Research* **2003,** *31* (14), 4001-4005.
37. Lechardeur, D.; Sohn, K. J.; Haardt, M.; Joshi, P. B.; Monck, M.; Graham, R. W.; Beatty, B.; Squire, J.; O'Brodovich, H.; Lukacs, G. L., Metabolic instability of plasmid DNA in the cytosol: a potential barrier to gene transfer. *Gene Therapy* **1999,** *6* (4), 482.
38. Bloomfield, V. A., DNA condensation by multivalent cations. In *Biopolymers*, 1997; Vol. 44, pp 269-282.
39. Bloomfield, V. A., DNA condensation. *Current Opinion in Structural Biology* **1996,** *6* (3), 334-341.
40. Mascotti, D. P.; Lohman, T. M., Thermodynamic Extent of Counterion Release Upon Binding Oligolysines to Single-Stranded Nucleic Acids. *Proceedings of the National Academy of Sciences of the United States of America* **1990,** *87* (8), 3142-3146.
41. Wagner, K.; Harries, D.; May, S.; Kahl, V.; Radler, J.; Ben-Shaul, A., Direct Evidence for Counterion Release upon Cationic Lipid-DNA Condensation. *Langmuir* **1999,** *16* (2), 303-306.
42. Boussif, O.; Zanta, M. A.; Mergny, M. D.; Scherman, D.; Demeneix, B.; Behr, J.-P., A Versatile Vector for Gene and Oligonucleotide Transfer into Cells in Culture and in vivo: Polyethylenimine. *Proceedings of the National Academy of Sciences of the United States of America* **1995,** *92* (16), 7297-7301.
43. Clamme, J. P.; Azoulay, J.; Mély, Y., Monitoring of the Formation and Dissociation of Polyethylenimine/DNA Complexes by Two Photon Fluorescence Correlation Spectroscopy. *Biophysical Journal* **2003,** *84* (3), 1960-1968.
44. Ogris, M.; Steinlein, P.; Kursa, M.; Mechtler, K.; Kircheis, R.; Wagner, E., The size of DNA/transferrin-PEI complexes is an important factor for gene expression in cultured cells. *Gene Therapy* **1998,** *5* (10), 1425-1433.
45. Xie, Q.; Xinyong, G.; Xianjin, C.; Yayu, W., PEI/DNA formation affects transient gene expression in suspension Chinese hamster ovary cells via a one-step transfection process. *Cytotechnology* **2013,** *65* (2), 263-271.

46. Singh, B.; Maharjan, S.; Park, T. E.; Jiang, T.; Kang, S. K.; Choi, Y. J.; Cho, C. S., Tuning the Buffering Capacity of Polyethylenimine with Glycerol Molecules for Efficient Gene Delivery: Staying In or Out of the Endosomes. *Macromolecular Bioscience* **2015,** *15* (5), 622-635.
47. Suh, J.; Wirtz, D.; Hanes, J., Efficient active transport of gene nanocarriers to the cell nucleus. *Proceedings of the National Academy of Sciences of the United States of America* **2003,** *100* (7), 3878-3882.
48. Behr, J. P., The proton sponge: A trick to enter cells the viruses did not exploit. *Chimia* **1997,** *51* (1-2), 34-36.
49. Garrett, R.; Grisham, C. M., What Are Viruses? In *Biochemistry*, 3 ed.; Thomson Brooks/Cole: Belmont, CA, **2005**; pp 26-27.
50. Gabrielson, N. P.; Pack, D. W., Efficient polyethylenimine-mediated gene delivery proceeds via a caveolar pathway in HeLa cells. *Journal of Controlled Release* **2009,** *136* (1), 54-61.
51. Won, Y.-Y.; Sharma, R.; Konieczny, S. F., Missing pieces in understanding the intracellular trafficking of polycation/DNA complexes. *Journal of Controlled Release* **2009,** *139*, 88-93.
52. Merdan, T.; Kunath, K.; Fischer, D.; Kopecek, J.; Kissel, T., Intracellular Processing of Poly(Ethylene Imine)/Ribozyme Complexes Can Be Observed in Living Cells by Using Confocal Laser Scanning Microscopy and Inhibitor Experiments. *Pharmaceutical Research* **2002,** *19* (2), 140-146.
53. Benjaminsen, R. V.; Mattebjerg, M. A.; Henriksen, J. R.; Moghimi, S. M.; Andresen, T. L., The Possible "Proton Sponge " Effect of Polyethylenimine (PEI) Does Not Include Change in Lysosomal pH. *Molecular Therapy* **2012,** *21* (1), 149.
54. Karatekin, E.; Sandre, O.; Brochard-wyart, F., Transient pores in vesicles. *Polymer International* **2003,** *52*, 486-493.
55. Bieber, T.; Meissner, W.; Kostin, S.; Niemann, A.; Elsasser, H.-P., Intracellular route and transcriptional competence of polyethylenimine–DNA complexes. *Journal of Controlled Release* **2002,** *82* (2), 441-454.
56. Hong, S.; Bielinska, A. U.; Mecke, A.; Keszler, B.; Beals, J. L.; Shi, X.; Balogh, L.; Orr, B. G.; Baker, J. R.; Banaszak Holl, M. M., Interaction of Poly(amidoamine) Dendrimers with Supported Lipid Bilayers and Cells: Hole Formation and the Relation to Transport. *Bioconjugate Chemistry* **2004,** *15* (4), 774-782.
57. Erich, A. N., Nucleocytoplasmic transport: signals, mechanisms and regulation. *Nature* **1997,** *386* (6627), 779.
58. Dworetzky, S. I.; Lanford, R. E.; Feldherr, C. M., The effects of variations in the number and sequence of targeting signals on nuclear uptake. *The Journal of Cell Biology* **1988,** *107* (4), 1279.
59. Clamme, J.-P.; Krishnamoorthy, G.; Mély, Y., Intracellular dynamics of the gene delivery vehicle polyethylenimine during transfection: investigation by two-photon fluorescence correlation spectroscopy. *Biochimica et Biophysica Acta (BBA) - Biomembranes* **2003,** *1617* (1–2), 52-61.
60. Dean, D. A.; Strong, D. D.; Zimmer, W. E., Nuclear entry of nonviral vectors. *Gene Therapy* **2005,** *12* (11), 881.

61. Fasbender, A.; Zabner, J.; Zeiher, B. G.; Welsh, M. J., A low rate of cell proliferation and reduced DNA uptake limit cationic lipid-mediated gene transfer to primary cultures of ciliated human airway epithelia. *Gene Therapy* **1997,** *4* (11), 1173.
62. Brunner, S.; Sauer, T.; Carotta, S.; Cotten, M.; Saltik, M.; Wagner, E., Cell cycle dependence of gene transfer by lipoplex, polyplex and recombinant adenovirus. *Gene Therapy* **2000,** *7* (5), 401.
63. Schaffer, D.; Fidelman, N.; Dan, N.; Lauffenburger, D., Vector unpacking as a potential barrier for receptor-mediated polyplex gene delivery. *Biotechnology and Bioengineering* **2000,** *67* (5), 598-606.
64. Huth, S.; Hoffmann, F.; von Gersdorff, K.; Laner, A.; Reinhardt, D.; Rosenecker, J.; Rudolph, C., Interaction of polyamine gene vectors with RNA leads to the dissociation of plasmid DNA-carrier complexes. *The Journal of Gene Medicine* **2006,** *8* (12), 1416-1424.
65. Thomas, M.; Klibanov, A., Non-viral gene therapy: polycation-mediated DNA delivery. *Applied Microbiology and Biotechnology* **2003,** *62* (1), 27-34.
66. Khansarizadeh, M.; Mokhtarzadeh, A.; Rashedinia, M.; Taghdisi, S. M.; Lari, P.; Abnous, K. H.; Ramezani, M., Identification of possible cytotoxicity mechanism of polyethylenimine by proteomics analysis. *Human & Experimental Toxicology* **2016,** *35* (4), 377-387.
67. Fischer, D.; Li, Y.; Ahlemeyer, B.; Krieglstein, J.; Kissel, T., In vitro cytotoxicity testing of polycations: influence of polymer structure on cell viability and hemolysis. *Biomaterials* **2003,** *24* (7), 1121-1131.
68. Plank, C.; Mechtler, K.; Szoka, F.; Wagner, E., Activation of the complement system by synthetic DNA complexes: A potential barrier for intravenous gene delivery. *Human Gene Therapy* **1996,** *7* (12), 1437-1446.
69. Dash, P. R.; Read, M. L.; Barrett, L. B.; Wolfert, M. A.; Seymour, L. W., Factors affecting blood clearance and in vivo distribution of polyelectrolyte complexes for gene delivery. *Gene Therapy* **1999,** *6* (4), 643.
70. Skoog, D. A.; Holler, F. J.; Nieman, T. A., *Principles of Instrumental Analysis*. 5th ed ed.; Hardcourt Brace COllege Publishers: Saunders College Pub.; Orlando, Fla. , 1998.
71. Hassan, P. A.; Rana, S.; Verma, G., Making Sense of Brownian Motion: Colloid Characterization by Dynamic Light Scattering. In *Langmuir*, **2015**; Vol. 31, pp 3-12.
72. Sudo, S.; Ohtomo, T.; Otsuka, K., Easy measurement and analysis method of zeta potential and electrophoretic mobility of water-dispersed colloidal particles by using a self-mixing solid-state laser. *Journal of Applied Physics* **2013,** *114* (6).
73. Warriner, L. W.; Duke, J. R.; Pack, D. W.; DeRouchey, J. E., Succinylated Polyethylenimine Derivatives Greatly Enhance Polyplex Serum Stability and Gene Delivery In Vitro. *Manuscript to be submitted for publication.* **2018**.
74. Roe, R. J., *Methods of X-ray and neutron scattering in polymer science*. New York: Oxford University Press: New York, 2000.
75. Eberhard, B., Introduction to x-ray scattering. *Journal of Physics: Condensed Matter* **2001,** *13* (34), 7477-7498.

76. Dong, Y.-D.; Boyd, B. J., Applications of X-ray scattering in pharmaceutical science. *International journal of pharmaceutics* **2011,** *417* (1), 101-111.
77. DeRouchey, J.; Netz, R. R.; Rädler, J. O., Structural investigations of DNA-polycation complexes. *The European Physical Journal E* **2005,** *16* (1), 17-28.
78. Skoog, D. A.; Holler, F. J.; Crouch, S. R., *Principles of instrumental analysis*. Brooks/Cole : Thomson Learning: Australia, **2007**.
79. Blanton, T. N.; Huang, T. C.; Toraya, H.; Hubbard, C. R.; Robie, S. B.; Louër, D.; Göbel, H. E.; Will, G.; Gilles, R.; Raftery, T., JCPDS—International Centre for Diffraction Data round robin study of silver behenate. A possible low-angle X-ray diffraction calibration standard. *Powder Diffraction* **2013,** *10* (2), 91-95.
80. Lee, B.; Lo, C. T.; Seifert, S.; Winans, R. E., Silver behenate as a calibration standard of grazing-incidence small-angle X-ray scattering. *Journal of Applied Crystallography* **2006,** *39* (5), 749-751.
81. An, M.; Hutchison, J. M.; Parkin, S. R.; DeRouchey, J. E., Role of pH on the Compaction Energies and Phase Behavior of Low Generation PAMAM–DNA Complexes. *Macromolecules* **2014,** *47* (24), 8768-8776.
82. Lieleg, O.; Ribbeck, K., Biological hydrogels as selective diffusion barriers. *Trends in Cell Biology* **2011,** *21* (9), 543-551.
83. Arends, F.; Baumgärtel, R.; Lieleg, O., Ion-specific effects modulate the diffusive mobility of colloids in an extracellular matrix gel. *Langmuir : the ACS journal of surfaces and colloids* **2013,** *29* (51), 15965-15973.
84. Li, Leon D.; Crouzier, T.; Sarkar, A.; Dunphy, L.; Han, J.; Ribbeck, K., Spatial Configuration and Composition of Charge Modulates Transport into a Mucin Hydrogel Barrier. *Biophysical Journal* **2013,** *105* (6), 1357-1365.
85. Lieleg, O.; Baumgärtel, R. M.; Bausch, A. R., Selective Filtering of Particles by the Extracellular Matrix: An Electrostatic Bandpass. *Biophysical Journal* **2009,** *97* (6), 1569-1577.
86. Zhang, X.; Hansing, J.; Netz, Roland R.; DeRouchey, Jason E., Particle Transport through Hydrogels Is Charge Asymmetric. *Biophysical Journal* **2015,** *108* (3), 530-539.
87. Banks, D. S.; Tressler, C.; Peters, R. D.; Hfling, F.; Fradin, C., Characterizing anomalous diffusion in crowded polymer solutions and gels over five decades in time with variable-lengthscale fluorescence correlation spectroscopy. *Soft Matter* **2016,** *12* (18), 4190-4203.
88. Derouchey, J.; Schmidt, C.; Walker, G. F.; Koch, C.; Plank, C.; Wagner, E.; Rädler, J. O., Monomolecular assembly of siRNA and poly(ethylene glycol)-peptide copolymers. *Biomacromolecules* **2008,** *9* (2), 724.
89. Michelman-Ribeiro, A.; Boukari, H.; Nossal, R.; Horkay, F., Structural changes in polymer gels probed by fluorescence correlation spectroscopy. *Macromolecules* **2004,** *37* (26), 10212-10214.
90. Shimizu, M.; Sasaki, S.; Tsuruoka, M., DNA length evaluation using cyanine dye and fluorescence correlation spectroscopy. *Biomacromolecules* **2005,** *6* (5), 2703-2707.
91. Tatarkova, S. A.; Kamra Verma, A.; Berk, D. A.; Lloyd, C. J., Quantitative fluorescence microscopy of macromolecules in gel and biological tissue. *Physics in Medicine and Biology* **2005,** *50* (23), 5759-5768.

92. Hansing, J.; Duke, J. R.; Fryman, E. B.; DeRouchey, J. E.; Netz, R. R., Diffusion in polymer gels with competing interaction sites. *Manuscript to be submitted for publication.* **2017**.
93. Gendron, P. O.; Avaltroni, F.; Wilkinson, K., Diffusion Coefficients of Several Rhodamine Derivatives as Determined by Pulsed Field Gradient–Nuclear Magnetic Resonance and Fluorescence Correlation Spectroscopy. *Journal of Fluorescence* **2008,** *18* (6), 1093-1101.
94. Elson, E. L.; Magde, D., Fluorescence correlation spectroscopy. I. Conceptual basis and theory. *Biopolymers* **1974,** *13* (1), 1-27.
95. Hess, S.; Huang, S.; Heikal, A. A.; Webb, W., Biological and chemical applications of fluorescence correlation spectroscopy: A review. In *Biochemistry*, **2002**; Vol. 41, pp 697-705.

VITA

Joseph Raleigh Duke III

PLACE OF BIRTH

Los Alamos, New Mexico

EDUCATION

B. S. in Biochemistry, Ogden College of Science and Engineering, Western Kentucky University, Bowling Green, KY, May 2014

PROFESSIONAL EXPERIENCE

Teaching Assistant, Department of Chemistry, University of Kentucky, Lexington, KY. August 2014 – May 2017

Research Assistant, University of Kentucky, Lexington, KY. June – August 2016, June – August 2017. Advisor: Dr. Jason DeRouchey.

Undergraduate Researcher, Western Kentucky University, Bowling Green, KY. May 2013 – May 2014. Advisor: Dr. Donald Slocum.

ACADEMIC HONORS

Presidents List (GPA of 3.8-4.0, WKU)

Scholar of the College (GPA of 4.0, WKU)

Outstanding Graduating Senior in Chemistry (2014, WKU)

WKU Honors College Student